REPORT DOCUMENTATION PAGE

Form Approved
OMB No. 0704-0188

1. REPORT DATE (DD-MM-YYYY)	2. REPORT TYPE	3. DATES COVERED
17/07/06	Final Report	May 1, 2003 - April 30, 2006

4. TITLE AND SUBTITLE
Genetically-Encoded Reporters of Signal Transduction

5a. CONTRACT NUMBER
N00014-03-1-0456

5b. GRANT NUMBER
N00014-03-1-0456

5c. PROGRAM ELEMENT NUMBER

6. AUTHOR(S)
Alice Ting

5d. PROJECT NUMBER

5e. TASK NUMBER

5f. WORK UNIT NUMBER

7. PERFORMING ORGANIZATION NAME(S) AND ADDRESS(ES)
Massachusetts Institute of Technology, Chemistry Dept.
77 Massachusetts Ave., Room 18-493
Cambridge, MA 02139

8. PERFORMING ORGANIZATION REPORT NUMBER

9. SPONSORING/MONITORING AGENCY NAME(S) AND ADDRESS(ES)
office of Naval Research
800 N. Quincy Street
Arlington, VA 22217-5000

10. SPONSOR/MONITOR'S ACRONYM(S)
ONR

11. SPONSOR/MONITOR'S REPORT NUMBER(S)

12. DISTRIBUTION/AILABILITY STATEMENT
Distribution Unlimited

DISTRIBUTION STATEMENT A
Approved for Public Release
Distribution Unlimited

13. SUPPLEMENTARY NOTES

14. ABSTRACT
please see attached sheet

15. SUBJECT TERMS
please see attached sheet

16. SECURITY CLASSIFICATION OF:			17. LIMITATION OF ABSTRACT	18. NUMBER OF PAGES	19a. NAME OF RESPONSIBLE PERSON
a. REPORT	b. ABSTRACT	c. THIS PAGE			Alice Ting
Unclass.	Unclass.	Unclass.	UL	9	19b. TELEPHONE NUMBER (Include area code) (617) 258-0218

14. ABSTRACT

We have developed new reporters for imaging signal transduction events in living cells along two lines. First, we created new fluorescent reporters for imaging specific histone phosphorylation and methylation events in real time with high spatial resolution. Second, we developed new methodology for attaching a variety of biophysical probes (including organic fluorophores, quantum dots, and photoaffinity probes) to specific proteins in the cellular context. This methodology was used to image neuronal proteins such as the AMPA-type glutamate receptor and neuroligin at the single molecule level in living neurons. Such efforts should contribute to our understanding of the molecular mechanisms of learning and memory and perhaps provide insight into neurodegenerative diseases such as Alzheimer's and Parkinson's.

15. SUBJECT TERMS

imaging, fluorescence, reporters, protein labeling, neurons, synapse, AMPA receptor, neuroligin, chromatin, histone phosphorylation, histone methylation, quantum dots, single-molecule

Cover page

Grant #: **N00014-03-1-0456**
Principal Investigator: **Alice Y. Ting**
Institution: **Massachusetts Institute of Technology**
Grant Title: **Genetically-Encoded Reporters of Signal Transduction**
Award Period: **5/1/2003 – 7/31/2006**

Objective

To develop fluorescent reporters for imaging signal transduction events in single living cells.

Approach

We have taken two separate approaches: (1) we have developed genetically-encoded reporters for reading out histone phosphorylation and methylation levels from single living cells. Because histone phosphorylation/methylation levels are closely tied to transcriptional regulation of particular genes, our reporters provide a method to visualize the first control point for gene expression in living cells. (2) we have developed hybrid genetically-encoded/small-molecule methods for attaching a wide range of probes (including organic fluorophores, quantum dots, and photoaffinity probes) to specific proteins in the live cell context. These probes have contributed a great deal to our understanding of protein structure and function *in vitro*, but have rarely been used in the live cell context, due to a lack of viable methods for targeting them to particular proteins with high specificity. Our probe targeting methods, which all employ enzyme ligases to achieve high sequence specificity, allow the non-invasive study of protein behavior within their native context of the live cell.

Accomplishments

Part I. Genetically-encoded fluorescent reporters for imaging histone phosphorylation and methylation events in single living cells.

Reporters for two enzyme classes (kinases and methyltransferases) have been developed and characterized (Lin et al. *JACS* 2004 and Lin et al. *Angew. Chem.* 2004). These reporters are four-part chimeric proteins consisting of (from N- to C-terminus) cyan fluorescent protein (CFP), a natural binding domain specific for the modification catalyzed by the enzyme of interest, a peptide substrate for the enzyme of interest, and yellow fluorescent protein (YFP). Modification of the substrate by phosphorylation or methylation allows it to form an intramolecular complex with the modification-specific binding domain, increasing FRET between the two flanking fluorescent proteins. Removal of the modification by the appropriate enzyme (phosphatase or demethylase) reverses the FRET change.

These reporters are easy to use (they can be introduced into cells by simple transfection) and provide a simple real-time optical readout of cell state. For instance, healthy cells may be easily distinguished from diseased cells overexpressing or lacking a particular kinase, acetyltransferase, or methyltransferase enzyme (common markers for certain types of cancer). Moreover, these reporters may potentially be useful in reporting cellular state changes in response to external stimuli such as chemical and biological warfare (CBW) agents.

We used our reporters to probe histone modification patterns during the process of mammalian cell division. An increase in FRET was observed in an H3 phosphorylation reporter localized to the nucleus of a HeLa cell just before dissolution of the nuclear membrane and separation of the two newly-formed nuclei. After cell division, the FRET level returned to its basal state.

Part II. Site-specific protein labeling with biophysical probes using enzyme ligases.

Many small-molecule and inorganic probes such as xanthene fluorophores, quantum dots, and photoaffinity labels, offer important advantages over GFP, such as smaller size, increased brightness, or increased functionality, but a major bottleneck to their routine use in cells is the lack of ability to target them with very high specificity to particular proteins of interest. A major focus of our research has been to develop new chemistries to target these non-genetically encodable probes to specific cellular proteins. In one approach, we have capitalized on the *E. coli* enzyme biotin ligase (BirA), which site-specifically ligates biotin to a lysine sidechain with a 15-amino acid recognition sequence called the "acceptor peptide" (AP). Graduate student Irwin Chen found that BirA could accept a ketone isostere in place of biotin, ligating this analog to AP fusion proteins. The ketone can then be derivatized selectively using hydrazide or hydroxylamine functionalized probes. Irwin labeled AP fusion proteins *in vitro*, in cell lysate, and on the surface of live mammalian cells using fluorophores and photoaffinity probes using this method (Chen et al. *Nature Methods* 2005).

We are also exploring the use of other enzymes for targeting small-molecule probes. Chi-Wang Lin, for example, found that transglutaminase could be used to label cell surface proteins fused to glutamine-containing recognition sequences with cadaverine-functionalized probes such as biotin and Alexaflour (Lin et al, *JACS* 2006).

Quantum dots are powerful probes that open up entirely new applications in imaging. They are 30-100 times brighter than the brightest organic fluorophores and never photobleach, making them ideal for routine single-molecule imaging in live cells. Because of their brightness and excellent two-photon cross sections they are also well-suited to tissue and *in vivo* imaging. Finally, quantum dots are electron dense and relatively large (5-20 nm) and thus the same labeled sample can be visualized by both optical and electron microscopy, offering the advantages of both live cell imaging and super high spatial resolution (5-10 nm).

Streptavidin-conjugated quantum dots are commercially available and thus a straightforward way to target quantum dots in the live cell context is to site-specifically biotinylate AP fusion proteins with biotin ligase. Dr. Mark Howarth demonstrated that this method of quantum dot targeting is fast, specific, and sensitive (offering many advantages over antibody-based targeting) and can be used to image and track single molecules of the AMPA-type glutamate receptor (Howarth et al, *PNAS* 2005) and the synaptic adhesion protein neuroligin. We are continuing our collaborations with Yasunori Hayashi (MIT) and Alaa El-Husseini (UBC) to gain insight into the molecular mechanisms of glutamate receptor and neuroligin trafficking in the processes of synaptic activation and synaptogenesis.

Mark Howarth is currently working to improve this biotin ligase-mediated targeting method by controlling quantum dot valency (ideally, each quantum dot should have a single biotin binding site so that cell surface proteins cannot be crosslinked during labeling) and reducing quantum dot size. For the first goal, Mark engineered a streptavidin heterotetramer with a single femtomolar biotin binding site (Howarth et al. *Nature Methods* 2006). He has also developed a protocol to perform mono-conjugation of these engineered streptavidins to quantum dots and has obtained quantum dots that are >90% monovalent. For the second goal, we have initiated a collaboration with Moungi Bawendi (MIT) to develop and use quantum dots with thinner coatings which significantly reduce their hydrodynamic radii. These smaller dots should help reduce

biological artifacts associated with addition of a large payload to cellular proteins and steric exclusion from spatially restricted sites such as the synapse (40 nm).

Conclusions

New methodologies have been developed to image signal transduction events in living cells:

- fluorescent reporters for imaging histone phosphorylation in living cells
- fluorescent reporters for imaging histone methylation in living cells
- site-specific labeling of recombinant cell surface proteins using transglutaminase
- site-specific labeling of recombinant cell surface proteins using biotin ligase and a ketone analog of biotin
- attaching quantum dots to specific cell surface proteins using quantum dots

These methods have allowed us to investigate several biological problems:

- real-time trafficking of single AMPA receptor molecules on the surface of living neurons; the relationship between AMPA receptor trafficking and synaptic plasticity
- real-time trafficking of single transferrin receptor molecules on the surface of living cells; differentiation between two competing models of clathrin-mediated internalization of the transferrin receptor: receptor activation triggers recruitment and formation of a clathrin-coated pit vs. activated receptors travel to pre-formed clathrin-coated pits
- real-time trafficking of neurexin and neuroligin clusters in living neurons; implications for the molecular mechanism of new synapse formation

Significance

The methods we have developed will be generally useful to cell biologists interested in studying protein function non-invasively in the live cell context. Our histone modification reporters will be useful to biologists wishing to image the early biochemical events that regulate transcription of specific genes. Unlike conventional biochemical methods, such as immunoprecipitation and immunofluorescence staining, our live cell reporters provide a real-time readout of biochemical events with high spatial resolution. Our site-specific labeling methods provide biologists with a general strategy to image and probe the trafficking and behavior of cell surface proteins. Biologists can fuse a peptide recognition sequence to their protein of interest, and then use either biotin ligase or transglutaminase to specifically attach a fluorophore, quantum dot, or photoaffinity probe. These probes offer major advantages over the conventionally-used tag, GFP, in that they can be smaller in size, brighter/more photostable, or provide functional readout (protein-protein interactions) as opposed to serving merely as a passive marker.

We are beginning to use these new methods ourselves, and in collaboration with other labs, to gain insight into mechanisms of receptor trafficking and their roles in important processes such as synaptic plasticity (crucial in learning and memory), new synapse formation, and nutrient uptake. Basic knowledge gained in these areas should aid in the development of new medicines and also help create cell-state specific biosensors and diagnostics.

Patent Information

Five patent applications have been filed from work supported by this grant.

Howarth, M. R.; Ting, A. Y. "Monovalent streptavidin with a single femtomolar biotin binding site" U. S. patent application no. 60/731166 (filed October 28, **2005**).

Howarth, M. R.; Ting, A. Y. "Monovalent avidin and streptavidin compositions." U. S. patent application no. 11/262325 (filed October 28, **2005**).

Chen, I.; Ting, A. Y. "Methods and compositions for peptide and protein labeling." U. S. patent application no. 11/040833 (published January 20, **2005**).

Ting, A. Y. "Site-specific labeling of recombinant proteins with an engineered fluorophore transferase." U. S. patent application no. 10/754911 (published January 9, **2004**).

Ting, A. Y. "Genetically-encoded fluorescent reporters of kinase, acetyltransferase, and methyltransferase activities." U. S. patent application no. 10/634740 (published August 5, **2003**).

Award Information

Distinctions obtained during the period covered by this grant include:

Camille Dreyfus Teacher-Scholar Award (2006)
McKnight Technological Innovations in Neuroscience Award (2005)
Alfred P. Sloan Foundation Research Fellowship (2005)
EJLB Foundation Scholar Research Program Award (2003)
National Institutes of Health Career Development Award (2003)

Publications (for total period of grant)

1. Lin, C.-W.; Ting, A. Y. "Transglutaminase-catalyzed site-specific conjugation of small-molecule probes to proteins *in vitro* and on the surface of live cells," *J. Am. Chem. Soc.* **2006**, *128*, 4542-4543.

2. Howarth, M.; Chinnapen, D. J.-F.; Gerrow, K.; Dorrestein, P. C.; Grandy, M. R.; Kelleher, N. L.; El-Husseini, A.; Ting, A. Y. "A monovalent streptavidin with a single femtomolar biotin binding site," *Nature Methods* **2006**, *3*, 267-273.

3. Howarth, M.; Takao, K.; Hayashi, Y.; Ting, A. Y. "Targeting quantum dots to surface proteins in living cells with biotin ligase," *Proc. Natl. Acad. Sci.* **2005**, *102*, 7583-7588.

4. Chen, I.; Howarth, M.; Lin, W.; Ting, A. Y. "Site-specific labeling of cell surface proteins with biophysical probes using biotin ligase," *Nature Methods* **2005**, *2*, 99-104.

5. Lin, C.-W.; Ting, A. Y. "A genetically-encoded fluorescent reporter of histone phosphorylation in living cells," *Angew. Chem. Int. Ed.* **2004**, *43*, 2940-2943.

6. Lin, C.-W.; Jao, C. Y.; Ting, A. Y. "Genetically-encoded fluorescent reporters of histone methylation in living cells," *J. Am. Chem. Soc.* **2004**, *126*, 5982-5983.

J|A|C|S
COMMUNICATIONS

Published on Web 03/16/2006

Transglutaminase-Catalyzed Site-Specific Conjugation of Small-Molecule Probes to Proteins in Vitro and on the Surface of Living Cells

Chi-Wang Lin and Alice Y. Ting*

Department of Chemistry, Massachusetts Institute of Technology, Cambridge, Massachusetts 02139

Received January 19, 2006; E-mail: ating@mit.edu

Compared to green fluorescent protein (GFP), non-genetically encoded probes, such as organic dyes and inorganic nanoparticles, offer the possibility of smaller probe sizes and access to a much wider array of functionality, from photocrosslinking and photoregulation to imaging of cellular processes by nonoptical methods, such as electron microscopy, magnetic resonance imaging, and positron emission tomography. The major limitation to the use of these probes in cells, however, is the shortage of robust methods for targeting them to specific proteins of interest. Recently, many new methodologies for protein labeling in cells have been reported.[1-3] Most of these use special peptide or protein handles, which are genetically fused to the target protein and recruit the probe of interest via a covalent or noncovalent interaction. There is great variation among these methods in terms of labeling specificity, speed, stability, tag size, toxicity, and versatility for probe structure and cell type, and no single method yet excels in all these respects. Thus new methods are still needed to facilitate the routine use of non-genetically encoded probes in the cellular context.

Transglutaminases (TGases) are enzymes that catalyze amide bond formation between glutamine and lysine side chains, with the loss of ammonia (Figure 1). They are ubiquitous in multicellular organisms and function in protein cross-linking events in migration, apoptosis, and wound healing, as well as in physiological disorders, such as Huntington's disease and Celiac Sprue.[4-6] One of the most well-studied TGases is the guinea pig liver transglutaminase (gpTGase), which is a 77 kD monomeric protein expressed in the cytosol.[5,7] gpTGase has unique properties which make it ideal for protein labeling applications. It exhibits high specificity for its glutamine-containing protein substrate, but wide tolerance for the structure of the amine-containing substrate.[8] Instead of lysine, amines as diverse as fluorescein cadaverine[9] and biotin cadaverine[10] can be utilized by gpTGase. Also, peptide substrates have been found which are efficiently modified by gpTGase both in isolation and when fused to recombinant proteins.[11,12] gpTGase has previously been used to label Q-tagged proteins in vitro; for instance, interleukin-2 and glutathione *S*-transferase have been tagged with monodansyl cadaverine[11] and fluorescein cadaverine,[12] respectively. However, the use of TGases for labeling specific Q-tagged proteins in cells or complex mixtures has never been reported.

We selected three Q-tag substrates of gpTGase and appended them to the N-terminus of cyan fluorescent protein (CFP). The Q1 (PNPQLPF),[13] Q2 (PKPQQFM),[11,12] and Q3 (GQQQLG)[14] fusions to CFP were each labeled efficiently (~70−80% labeling extent, data not shown) and specifically (alanine mutations within the Q-tags suppressed labeling by 3−17-fold) by purified gpTGase with fluorescein cadaverine in vitro (Figure S1). To test gpTGase for labeling of cell surface proteins (Figure 1), we expressed each Q-tag CFP fusion on the surface of HeLa and labeled with either biotin cadaverine (followed by streptavidin−Alexa 568 conjugate for detection) or Alexa 568 cadaverine directly. Both probes were successfully conjugated to all three Q-tags, and Figure 2 shows

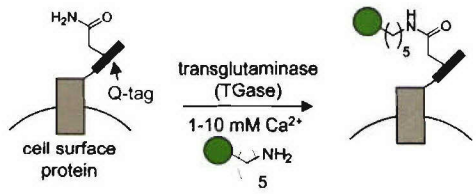

Figure 1. Transglutaminase-catalyzed ligation of cadaverine-functionalized probes (green circle) to Q-tag-fused recombinant cell surface proteins. TGase ligates the glutamine side chain of the Q-tag (blue) to the amine probe, giving an amide bond and releasing ammonia. In this study, three Q-tag peptide substrates were used: Q1 (PNPQLPF), Q2 (PKPQQFM), and Q3 (GQQQLG).

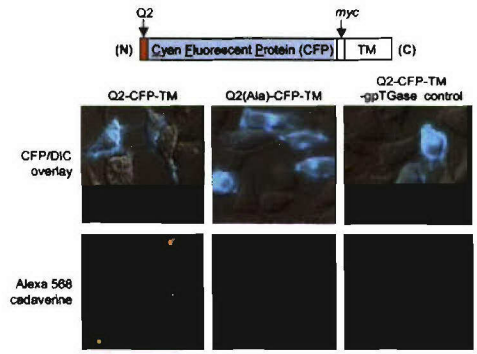

Figure 2. TGase-catalyzed labeling of a Q-tagged cell surface protein. The domain structure of Q2-CFP-TM is shown. TM is the transmembrane domain of the PDGF receptor, which targets Q2-CFP to the cell surface. HeLa expressing Q2-CFP-TM were labeled with Alexa 568 cadaverine by incubating with the probe, gpTGase, and 12 mM $CaCl_2$ for 25 min at 4 °C. The top row shows the CFP images superimposed on the DIC images. The bottom row shows the Alexa 568 fluorescence. Negative controls are shown with the alanine mutant Q2(Ala)-CFP-TM or with gpTGase enzyme omitted.

that Alexa 568 conjugation to Q2 was both site-specific (signal to background ratio ranged from 2.5−6) and enzyme-dependent. Biotin cadaverine conjugation to Q3-tagged epidermal growth factor receptor (EGFR) was also successful (Figure S2), and labeling did not impair receptor response to EGF (data not shown). As an additional test of the potential cytotoxicity of the labeling conditions, we monitored the intracellular Ca^{2+} levels using calcium Green-1[15] and observed no change during labeling (data not shown). HeLa growth rate was also unaffected 24 h after labeling.

We also assessed the specificity of labeling by immunoblot (Figure S3). Living cells expressing Q2-CFP targeted to the cell surface (Q2-CFP-TM, Figure 2) were labeled with biotin cadaverine and then lysed. The lysate was run on SDS−PAGE and blotted with streptavidin. A single biotinylated band was observed at the molecular weight of Q2-CFP-TM (37 kD). The band disappeared when the alanine mutant of Q2-CFP-TM was used instead, or when gpTGase was omitted from the labeling reaction.

To demonstrate the utility of TGase-mediated site-specific labeling, we investigated the homodimerization of the NF-κB

10.1021/ja0604111 CCC: $33.50

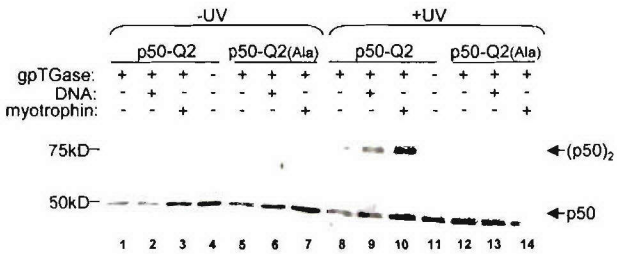

Figure 3. Labeling p50-Q2 with benzophenone and photoinduced cross-linking. The p50-Q2 protein was labeled with benzophenone spermine using gpTGase and $CaCl_2$ for 1.5 h at 37 °C. After Ni−NTA purification to remove excess benzophenone, the protein was irradiated with UV light for 7 min at 4 °C, in the presence or absence of DNA (0.18 μM) or myotrophin (360 μM; 90 equiv over p50).[21] The products were separated on 10% SDS−PAGE and blotted with anti-p50 antibody. Formation of p50 dimer (MW 78.5 kD) is elevated in lanes 8−10.

transcription factor p50, which binds to DNA and acts as a transcriptional repressor in its homodimeric form.[16] The most popular assay for determining the quantity of p50 homodimer in vitro and in cell lysates is the electrophoretic mobility shift assay (EMSA).[17] However, this assay can be both tedious and inaccurate because the DNA probe used for EMSA can itself change the percent of homodimer and p50 can dissociate from DNA within the gel. We synthesized a benzophenone spermine photoaffinity probe (Figure S4) and ligated it to p50-Q2 through incubation with gpTGase and calcium for 1.5 h at 37 °C. Excess probe was removed by nickel affinity purification. After irradiation with UV light, p50-Q2 monomer and covalently cross-linked homodimer were separated on SDS−PAGE and detected with anti-p50 antibody (Figure 3). We found that formation of the p50 homodimer increased in the presence of DNA, consistent with previous reports.[18,19] We also tested the effect of the protein myotrophin, which is similar in structure to IκBα and has previously been shown to promote p50 homodimerization.[20,21] We observed that myotrophin alone, without DNA, was sufficient to substantially increase the concentration of p50 homodimer. This illustrates one advantage of the photocrosslinking assay compared to EMSA, namely, that it is possible to probe the effect of additives on homodimer levels in the absence of DNA.

A trend that has emerged from existing labeling techniques is that there is a tradeoff between labeling specificity and tag size. Methods that use peptide tags to direct probes, such as FlAsH,[22] are generally less specific than methods that use protein tags, such as FKBP.[23] One way to circumvent this problem is to use enzymes to mediate the tag−probe interaction, as we have previously done with biotin ligase.[24,25] The excellent peptide specificity of this labeling technique derives from the natural specificity of biotin ligase. However, in its present form, the versatility of biotin ligase labeling is limited because the enzyme is extremely specific for the biotin structure and major active site re-engineering is required to incorporate probes with little structural similarity to biotin. The TGase labeling method described here, which is highly versatile for probe structure, is superior to biotin ligase labeling in this respect.

It is unlikely that TGase labeling can be extended to tagging of intracellular proteins because of competition from endogenous TGase substrates and because intracellular calcium concentrations under basal conditions are too low for TGase activity. In addition, gpTGase's specificity for the Q-tag is not extremely high, so that under forcing conditions we observed labeling of non-Q-tagged proteins. This contrasts with the exceptional peptide specificity of biotin ligase.[24,25] However, through optimization of labeling conditions, we were able to achieve highly specific labeling of the Q-tag both in vitro and on live cell surfaces, within relatively short time scales. In future work, we plan to investigate the use of factor XIIIa transglutaminase for labeling, which is known to exhibit higher sequence specificity than gpTGase.[26] We developed an assay for detection of NF-κB homodimers that provides some advantages over the commonly used EMSA assay. We plan to further refine the NF-κB assay and explore the use of TGase labeling for the study of protein trafficking and cell−cell interactions.

Acknowledgment. This work was supported by MIT, NIH (1 P20 GM072029-01), ONR (N00014-03-1-0456), the Sloan Foundation, and the Dreyfus Foundation (New Faculty Award). C.-W. L. was supported by a Merck/MIT fellowship. We thank Jeremy A. Ryan for technical assistance, Marta Fernandez-Suarez for myotrophin and helpful suggestions, and Jeff Keillor for the Q1-tag sequence.

Supporting Information Available: Experimental procedures for the preparation of all Q-tag constructs, labeling conditions in vitro and on living cells, benzophenone spermine synthesis, and the photocrosslinking assay for p50. This material is available free of charge via the Internet at http://pubs.acs.org.

References

(1) Chen, I.; Ting, A. Y. *Curr. Opin. Biotechnol.* **2005**, *16*, 35−40.
(2) Miller, L. W.; Sable, J.; Goelet, P.; Sheetz, M. R.; Cornish, V. W. *Angew. Chem., Int. Ed.* **2004**, *43*, 1672−1675.
(3) Johnsson, N.; George, N.; Johnsson, K. *Chembiochem* **2005**, *6*, 47−52.
(4) Bruce, S. E.; Bjarnason, I.; Peters, T. J. *Clin. Sci.* **1985**, *68*, 573−579.
(5) Greenberg, C. S.; Birckbichler, P. J.; Rice, R. H. *FASEB J.* **1991**, *5*, 3071−3077.
(6) Lorand, L.; Graham, R. M. *Nat. Rev. Mol. Cell Biol.* **2003**, *4*, 140−156.
(7) Connellan, J. M.; Chung, S. I.; Whetzel, N. K.; Bradley, L. M.; Folk, J. E. *J. Biol. Chem.* **1971**, *246*, 1093−1098.
(8) Lorand, L.; Parameswaran, K. N.; Stenberg, P.; Tong, Y. S.; Velasco, P. T.; Jonsson, N. A.; Mikiver, L.; Moses, P. *Biochemistry* **1979**, *18*, 1756−1765.
(9) Wolff, C.; Lai, C. S. *Biochemistry* **1988**, *27*, 3483−3487.
(10) Slaughter, T. F.; Achyuthan, K. E.; Lai, T S.; Greenberg, C. S. *Anal. Biochem.* **1992**, *205*, 166−171.
(11) Sato, H.; Ikeda, M.; Suzuki, K.; Hirayama, K. *Biochemistry* **1996**, *35*, 13072−13080.
(12) Taki, M.; Shiota, M.; Taira, K. *Protein Eng. Des. Sel.* **2004**, *17*, 119−126.
(13) Personal communication with J. Keillor.
(14) Hu, B. H.; Messersmith, P. B. *J. Am. Chem. Soc.* **2003**, *125*, 14298−14299.
(15) Mahoney, M. G.; Randall, C. J.; Linderman, J. J.; Gross, D. J.; Slakey, L. L. *Mol. Biol. Cell* **1992**, *3*, 493−505.
(16) Chen, L. F.; Greene, W. C. *Nat. Rev. Mol. Cell Biol.* **2004**, *5*, 392−401.
(17) Fujita, T.; Nolan, G. P.; Ghosh, S.; Baltimore, D. *Genes Dev.* **1992**, *6*, 775−787.
(18) Phelps, C. B.; Sengchanthalangsy, L. L.; Malek, S.; Ghosh, G. *J. Biol. Chem.* **2000**, *275*, 24392−24399.
(19) Siebenlist, U.; Franzoso, G.; Brown, K. *Annu. Rev. Cell Biol.* **1994**, *10*, 405−455.
(20) Sivasubramanian, N.; Adhikary, G.; Sil, P. C.; Sen, S. *J. Biol. Chem.* **1996**, *271*, 2812−2816.
(21) Knuefermann, P.; Chen, P.; Misra, A.; Shi, S. P.; Abdellatif, M.; Sivasubramanian, N. *J. Biol. Chem.* **2002**, *277*, 23888−23897.
(22) Adams, S. R.; Campbell, R. E.; Gross, L. A.; Martin, B. R.; Walkup, G. K.; Yao, Y.; Llopis, J.; Tsien, R. Y. *J. Am. Chem. Soc.* **2002**, *124*, 6063−6076.
(23) Marks, K. M.; Braun, P. D.; Nolan, G. P. *Proc. Natl. Acad. Sci. U.S.A.* **2004**, *101*, 9982−9987.
(24) Chen, I.; Howarth, M.; Lin, W. Y.; Ting, A. Y. *Nat. Methods* **2005**, *2*, 99−104.
(25) Howarth, M.; Takao, K.; Hayashi, Y.; Ting, A. Y. *Proc. Natl. Acad. Sci. U.S.A.* **2005**, *102*, 7583−7588.
(26) Gorman, J. J.; Folk, J. E. *J. Biol. Chem.* **1981**, *256*, 2712−2715.

JA0604111

A monovalent streptavidin with a single femtomolar biotin binding site

Mark Howarth[1], Daniel J-F Chinnapen[1,4], Kimberly Gerrow[2,4], Pieter C Dorrestein[3], Melanie R Grandy[1], Neil L Kelleher[3], Alaa El-Husseini[2] & Alice Y Ting[1]

Streptavidin and avidin are used ubiquitously because of the remarkable affinity of their biotin binding, but they are tetramers, which disrupts many of their applications. Making either protein monomeric reduces affinity by at least 10^4-fold because part of the binding site comes from a neighboring subunit. Here we engineered a streptavidin tetramer with only one functional biotin binding subunit that retained the affinity, off rate and thermostability of wild-type streptavidin. In denaturant, we mixed a streptavidin variant containing three mutations that block biotin binding with wild-type streptavidin in a 3:1 ratio. Then we generated monovalent streptavidin by refolding and nickel-affinity purification. Similarly, we purified defined tetramers with two or three biotin binding subunits. Labeling of site-specifically biotinylated neuroligin-1 with monovalent streptavidin allowed stable neuroligin-1 tracking without cross-linking, whereas wild-type streptavidin aggregated neuroligin-1 and disrupted presynaptic contacts. Monovalent streptavidin should find general application in biomolecule labeling, single-particle tracking and nanotechnology.

Streptavidin and avidin bind the small molecule biotin with femtomolar affinity[1]. This tight and specific binding has caused the (strept)avidin-biotin system to be used widely for biomolecule labeling, purification, immobilization and patterning. But because streptavidin and avidin are both tetramers, they can tetramerize the biotin conjugates to which they bind. This multimerization can interfere with normal biomolecule function or trafficking, or complicate affinity measurements, limiting the applications of this system. Much effort has been made to develop monomeric (strept)avidin. Disruption of the tetramer interface is straightforward, but is always accompanied by a dramatic decrease in biotin affinity (at least 10^4-fold in the best case for streptavidin[2] and 10^8-fold for avidin[3,4]) because the biotin binding site lies at the interface between subunits[5,6]. An alternative approach to generate monovalent (strept)avidin is to titrate in three equivalents of biotin per tetramer, but this is unsatisfactory because it generates a statistical mixture of mono-, di-, tri- and tetravalent (strept)avidins (see **Supplementary Methods** online).

We recently reported the use of site-specific protein biotinylation and streptavidin labeling to image cellular proteins[7]. This method can be used to specifically tag proteins at the cell surface, requires genetic fusion of the protein of interest to only a 15-amino-acid peptide, provides a stable linkage that does not dissociate over hours and can be used for introduction of a wide range of probes, from organic fluorophores to quantum dots. We were concerned, however, that the streptavidin could cross-link biotinylated cell-surface proteins (such as the AMPA receptor used in our earlier study[7]), thus slowing their trafficking and causing unwanted receptor activation[8]. Here we report the development of a monovalent streptavidin with a single femtomolar biotin binding site, and its application to cross-linking–free labeling of biotinylated neuroligin-1 on the surface of living neurons.

RESULTS

Generation of monovalent streptavidin

Our strategy for producing monovalent streptavidin is shown in **Figure 1a**. We wanted to produce a streptavidin tetramer consisting of three subunits unable to bind biotin and one subunit that binds biotin as well as wild-type streptavidin. Many of the known mutations in streptavidin reduce biotin affinity dramatically[2,6,9] but still leave dissociation constant (K_d) values in the nanomolar range and disrupt tetramerization[2]. The double mutant N23A, S27D has one of the weakest reported affinities for biotin (K_d = 7×10^{-5} M)[10] while still remaining a tetramer. Nevertheless we observed that N23A, S27D streptavidin still bound to biotinylated cells (data not shown). We found that mutation of an additional amino acid in the biotin binding site yielded a triple mutant (N23A, S27D, S45A; **Fig. 1b**) with negligible biotin binding, but left the tetramer structure intact. The biotin affinity of this mutant (composed of 'dead' (D) subunits; **Fig. 1**) was so weak that it was difficult to measure, but we obtained an approximate K_d of 1.2×10^{-3} M. To generate monovalent streptavidin (**Fig. 1c**), we added a 6His tag to the wild-type subunit ('alive' (A) subunit; **Fig. 1**), then combined D and A subunits at a molar ratio of 3:1 in guanidinium hydrochloride and refolded them by rapidly diluting the mixture into phosphate buffered saline (PBS). This refold

[1]Department of Chemistry, Massachusetts Institute of Technology, Cambridge, Massachusetts 02139, USA. [2]Department of Psychiatry, the Brain Research Center, University of British Columbia, Vancouver, British Columbia V6T 1Z3, Canada. [3]Department of Chemistry, University of Illinois Urbana-Champaign, Urbana, Illinois 61801, USA. [4]These authors contributed equally to this work. Correspondence should be addressed to A.Y.T. (ating@mit.edu).

RECEIVED 11 NOVEMBER 2005; ACCEPTED 31 JANUARY 2006; PUBLISHED ONLINE 22 MARCH 2006; DOI:10.1038/NMETH861

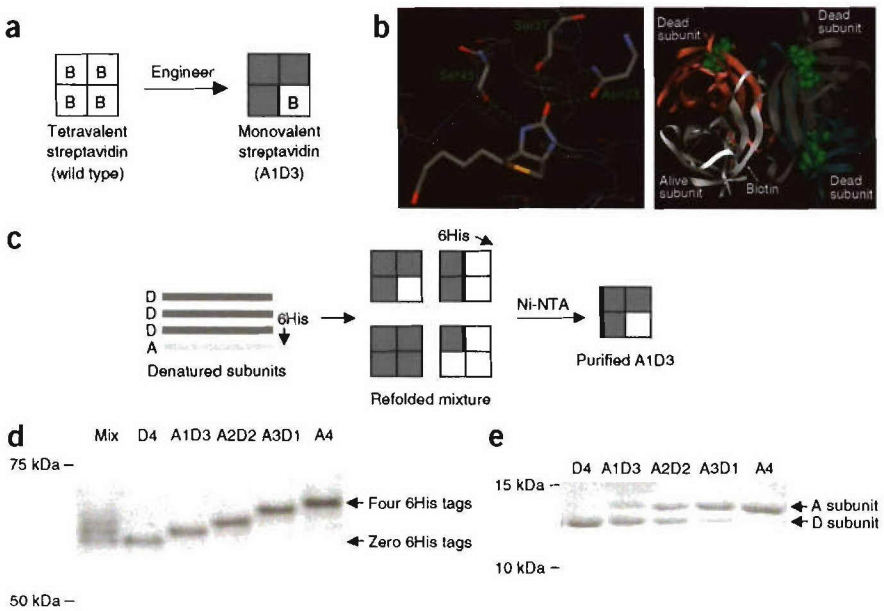

Figure 1 | Generation of monovalent streptavidin. (**a**) Wild-type streptavidin is a tetramer with four biotin binding sites (B, biotin). Monovalent streptavidin is a tetramer with 3 inactive subunits (dark gray) and one subunit that binds biotin with wild-type affinity (light gray). (**b**) Biotin binding site of wild-type streptavidin (from Protein Data Bank 1MK5)[11], highlighting the three residues mutated to create the 'dead' subunit (left). Asn23 and Ser45 were changed to alanines, removing two hydrogen bonds (dashed lines) to biotin, and Ser27 was changed to aspartate, to introduce a steric clash. In monovalent streptavidin, the residues mutated in the dead subunits are shown in green (right). (**c**) To make monovalent streptavidin, dead streptavidin subunits (D) and wild-type streptavidin subunits (A) in a 3:1 ratio were refolded from denaturant, giving a mix of streptavidin heterotetramers. Tetramers with a single 6His-tagged wild-type subunit were purified on a Ni-NTA column. (**d**) SDS-PAGE of chimeric streptavidins under nondenaturing conditions. Streptavidin with 4 dead subunits (D4), wild-type streptavidin with a 6His-tag (A4), the product of refolding of D and A in a 3:1 ratio (Mix), and chimeric tetramers with one (A1D3), two (A2D2) or three (A3D1) biotin binding subunits were loaded without boiling onto a polyacrylamide gel and visualized by Coomassie staining. (**e**) SDS-PAGE of chimeric streptavidins under denaturing conditions to break the tetramer into monomers.

generated a statistical mixture of tetramers of different composition. We purified the different tetramers using a nickel–nitrilotriacetic acid (Ni-NTA) column, eluting according to the number of 6His tags with increasing concentrations of imidazole. The tetramers could be distinguished by SDS-PAGE, if the samples were not boiled, according to the number of 6His tags present, showing that at least 30% of the initial mixture was of the monovalent A1D3 form (**Fig. 1d** and **Supplementary Methods**). Thus we obtained purified fractions of the monovalent A1D3 (final yield, 2 mg/l), as well as of the other chimeric streptavidins, A2D2 and A3D1. We confirmed the tetramer composition by boiling the samples before loading on SDS-PAGE, to determine the ratio of A to D subunits (**Fig. 1e**), and by electrospray ionization mass spectrometry (**Table 1** and **Supplementary Fig. 1** online). Despite the large mass of the streptavidin tetramer and the noncovalent interaction between subunits, we found good agreement between expected and observed masses for D4, A1D3, A2D2, A3D1 and A4.

Stability of monovalent streptavidin

We tested whether monovalent streptavidin would rearrange its subunit composition over time. We incubated A1D3 at 26 °C or at 37 °C and analyzed the reactions by SDS-PAGE to look for the appearance of D4 and A2D2 as a result of subunit exchange (**Fig. 2a**). No bands corresponding to D4 or A2D2 could be detected after incubation for up to one week. We did, however, detect a faint band, comprising ~3% of total protein and migrating faster than D4, after incubation at 26 °C for 1 week or at 37 °C for 1 d. This is most likely the result of a small degree of proteolysis of A1D3. Formation of A2D2 after incubation at 37 °C for 1 d was also not detected by silver staining, immunoblotting with an antibody to the 6His tag or mass spectrometry (data not shown). Thus substantial fractions of multivalent streptavidin will not be generated upon storage. We next tested the stability of A1D3 in terms of dissociation into monomers, as many mutations in the biotin binding site of streptavidin weaken tetramer stability[2]. We heated wild-type streptavidin and A1D3 in PBS at various temperatures for 3 min and determined tetramer disassembly by SDS-PAGE (**Fig. 2b**). A substantial fraction of A1D3 remained tetrameric even at 100 °C. There was little difference in thermostability between wild-type and monovalent streptavidin, suggesting that the mutations in D have minimal effect on the subunit interfaces, and that it should be possible to use A1D3 in assays requiring high temperatures.

Biotin binding by chimeric streptavidins

We used electrospray ionization mass spectrometry to determine the number of biotin molecules bound per tetramer. We acquired spectra of the different streptavidin tetramers with or without biotin. As expected, all four subunits of A4 were associated with biotin

Table 1 | Mass of different streptavidin tetramers with or without biotin

Tetramer	Predicted mass (without biotin)	Observed mass (without biotin)	Observed mass (with biotin)	Change in mass	Number of biotins bound
D4	52,962	52,997 ± 4	52,996 ± 12	−1 ± 2	0
A1D3	53,816	53,848 ± 5	54,088 ± 6	240 ± 4	1
A2D2	54,669	54,704 ± 6	55,193 ± 3	489 ± 4	2
A3D1	55,523	55,490 ± 45	56,201 ± 13	711 ± 39	3
A4	56,377	56,394 ± 8	57,378 ± 8	984 ± 7	4

The observed mass in daltons (±s.d.), determined by electrospray ionization mass spectrometry, is compared to the mass predicted from the sequence. From the change (±s.e.m.) upon addition of biotin (mass 244.31 Da), we determined how many biotin molecules were bound to each tetramer.

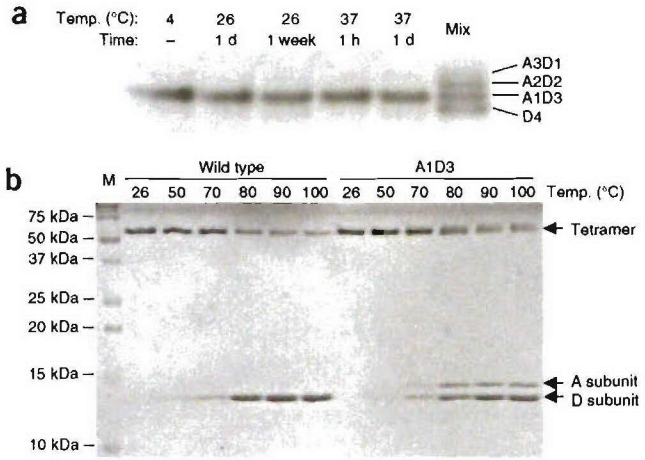

Figure 2 | Stability of monovalent streptavidin. (**a**) Stability to subunit exchange was determined by incubating 5 μM A1D3 in PBS as indicated, and detecting rearranged tetramers by 8% SDS-PAGE, by comparison to the initial product of refolding of D and A in a 3:1 ratio (Mix). (**b**) Stability of tetramer to heat denaturation was determined by incubating 5 μM wild-type streptavidin or A1D3 in PBS at the indicated temperatures for 3 min and then analyzing on 16% SDS-PAGE. M, marker.

(**Table 1** and **Supplementary Fig. 1**). No biotin binding by D4 could be detected. A1D3 was monovalent, binding a single biotin. The other chimeric tetramers bound one biotin per A subunit.

We determined the biotin binding affinity of the various streptavidin tetramers by measuring the competition with wild-type streptavidin for [^{3}H]biotin[9] (**Fig. 3**). The tetramer of dead subunits had negligible biotin binding, with an approximate K_d of $1.2 \times 10^{-3} \pm 0.2 \times 10^{-3}$ M (s.e.m.). The 6His tag did not affect biotin binding[9], as the measured affinity for A4 was $4.4 \times 10^{-14} \pm 1.1 \times 10^{-14}$ M (s.e.m.), similar to the untagged wild-type affinity of 4.0×10^{-14} M[1]. We determined a K_d of $4.8 \times 10^{-14} \pm 0.5 \times 10^{-14}$ M (s.e.m.) for monovalent A1D3 and a K_d of $5.4 \times 10^{-14} \pm 0.8 \times 10^{-14}$ M (s.e.m.) for divalent A2D2, indicating that the affinity of the chimeric tetramers for biotin was comparable to that of wild-type streptavidin.

We also evaluated the stability of biotin conjugate binding to A1D3 using an off-rate assay (**Fig. 3c**). As a positive control for biotin conjugate dissociation, we used a previously characterized streptavidin mutant with an accelerated off rate, S45A (ref. 11), and a streptavidin mutant that we found ourselves to have a fast off rate, T90I. The S45A and the T90I streptavidin mutants each showed >50% dissociation from a biotin-fluorescein conjugate in 1 h, whereas wild-type streptavidin and A1D3 both dissociated less than 10% in 12 h at 37 °C (**Fig. 3c**). A1D3 also had a comparable off rate to wild-type streptavidin for [^{3}H]biotin itself (**Fig. 3d**). The measured off rates were $5.2 \times 10^{-5} \pm 0.3 \times 10^{-5}$ s^{-1} (s.e.m.) for wild-type streptavidin and $6.1 \times 10^{-5} \pm 0.2 \times 10^{-5}$ s^{-1} (s.e.m.) for A1D3.

Labeling of cell-surface proteins without cross-linking

To test the use of monovalent streptavidin for labeling cell-surface proteins, we expressed cyan fluorescent protein (CFP) fused to a biotinylation sequence (the 'acceptor peptide'; AP) on the surface of HeLa cells using the transmembrane domain of platelet-derived

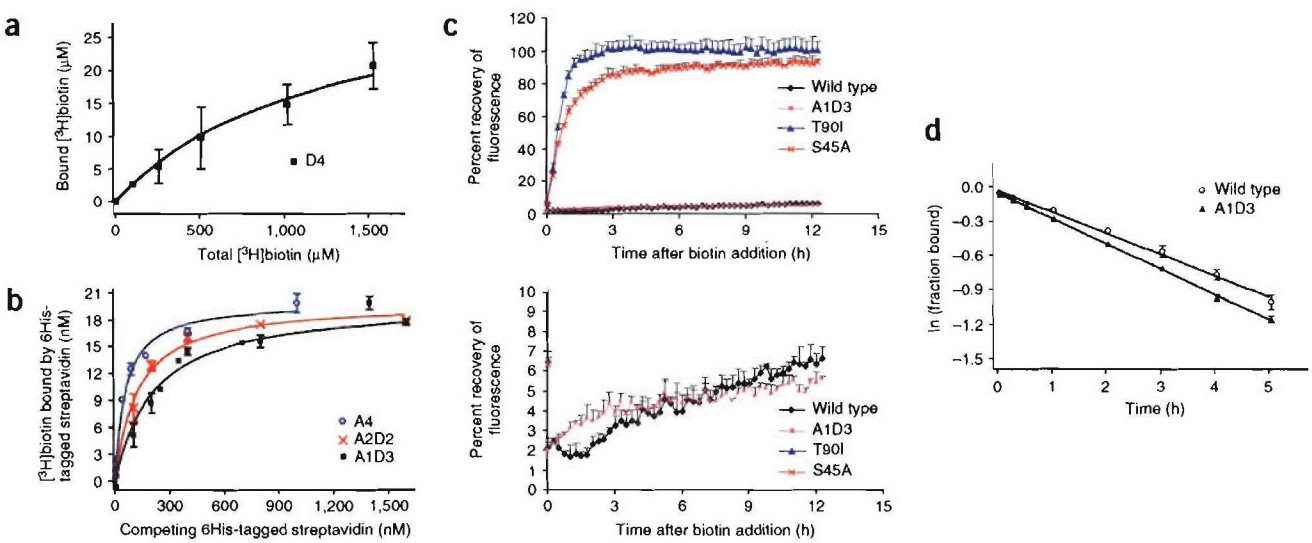

Figure 3 | Affinity and off rate of biotin binding to chimeric tetramers. (**a**) To determine the K_d for D4, 24 μM D4 was incubated with increasing concentrations of [^{3}H]biotin. After 20 h, the amount of bound [^{3}H]biotin was determined by precipitating D4. Means of triplicate measurements are shown ±1 s.d. Some error bars are too small to be visible. (**b**) To determine the K_d for A1D3, A2D2 and A4, increasing concentrations of A1D3, A2D2 or A4 were incubated with 20 nM [^{3}H]biotin and 50 nM wild-type streptavidin. After 20 h, chimeric tetramers were removed using Ni-NTA agarose, and the amount of [^{3}H]biotin bound to wild-type streptavidin in the supernatant was measured. From this value, the amount of [^{3}H]biotin bound to the chimeric tetramers was deduced. Means of triplicate measurements are shown ±1 s.d. (**c**) Off rate from a biotin conjugate. Wild-type, A1D3, S45A or T90I streptavidin was added in excess to biotin-4-fluorescein to quench its fluorescence. Excess competing biotin was added and fluorescence increase was monitored as biotin-4-fluorescein dissociated from streptavidin. The 100% value represents complete dissociation of biotin-4-fluorescein. Means of triplicate measurements are shown +1 s.d. The bottom panel is a magnification of the 0–10% region of the *y* axis, to illustrate the similar dissociation curves for wild-type streptavidin and A1D3. (**d**) Off rate from biotin. A1D3 or wild-type streptavidin was incubated with [^{3}H]biotin. Excess cold biotin was then added. After varying amounts of time at 37 °C, the amount of bound [^{3}H]biotin was determined by precipitating streptavidin. Means of triplicate measurement are shown ±1 s.d.

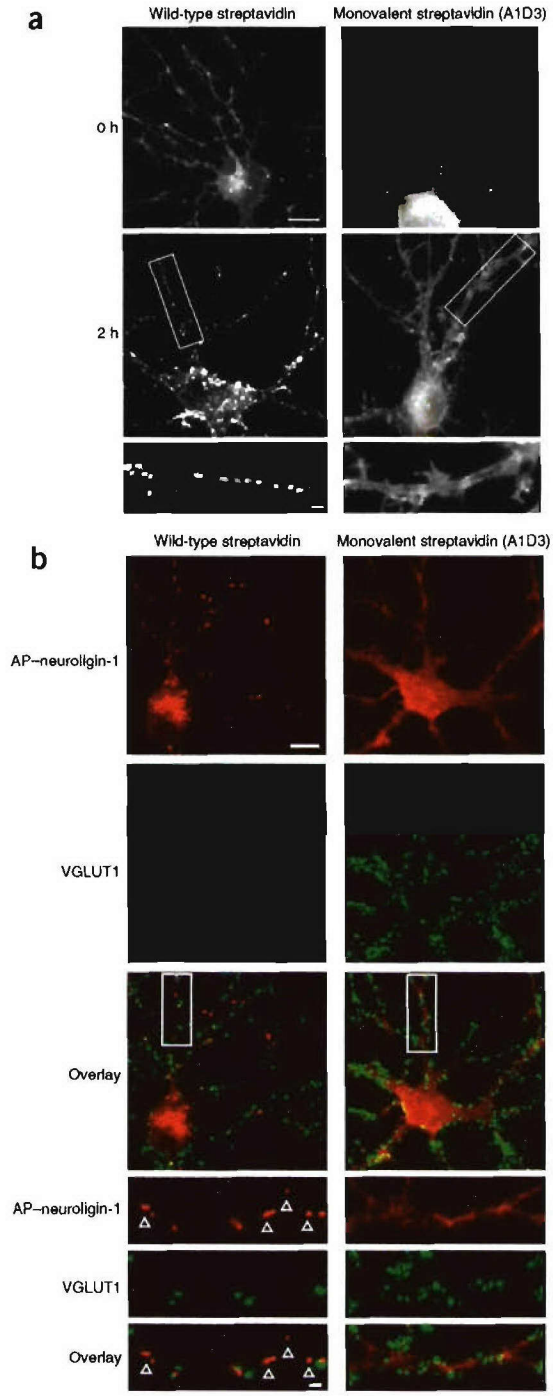

Figure 4 | Effect of monovalent and wild-type streptavidin on neuroligin-1 clustering. (**a**) Hippocampal neurons in dissociated culture were transfected with AP–neuroligin-1, biotinylated with biotin ligase and labeled with Alexa Fluor 568–conjugated wild-type (left) or A1D3 (right) streptavidin. After staining, cells were incubated for 0 h (top) or 2 h (middle) at 37 °C and streptavidin staining was visualized by live-cell fluorescence microscopy. Scale bar, 10 μm. Magnified images of the boxed regions are shown at the bottom. Scale bar, 1 μm. (**b**) Neurons were biotinylated and labeled with wild-type or A1D3 streptavidin as in **a**, incubated for 24 h and then stained for the presynaptic marker VGLUT1. Streptavidin (red) and VGLUT1 (green) signals are shown separately or overlaid. Scale bar, 10 μm. Magnified images of the boxed regions are shown below. Scale bar, 1 μm. Arrows indicate AP–neuroligin-1 clusters not apposed to presynaptic termini.

growth factor (PDGF) receptor (AP-CFP-TM)[12]. We biotinylated cell-surface acceptor peptide by incubation with extracellular biotin ligase and biotin-AMP for 10 min[7]. After washing the cells, we detected biotin with either wild-type or monovalent streptavidin, conjugated to Alexa Fluor 568. Detection was equally efficient and specific in both cases (**Supplementary Fig. 2** online). Incubating biotinylated cells with fluorescently labeled D4 tetramer gave no detectable staining, indicating that binding of A1D3 to biotinylated surface proteins should only occur through the A subunit.

We next tested whether labeling with monovalent streptavidin could prevent cross-linking of biotinylated cell-surface proteins, compared to wild-type streptavidin. Neuroligin-1 is a postsynaptic adhesion protein important in synapse formation[13]. Clustering of neuroligin-1 has been observed during synapse development and may depend upon interactions with the postsynaptic protein PSD-95 and the presynaptic binding partner neurexin[14,15]. We fused the extracellular N terminus of neuroligin-1 to an acceptor peptide tag and expressed this construct in dissociated hippocampal neurons. After adding biotin ligase to the cell medium and incubating for 5 min, we detected biotinylated AP–neuroligin-1 with either wild-type or monovalent streptavidin, conjugated to Alexa Fluor 568. Imaging immediately after labeling showed diffuse localization of AP–neuroligin-1 in both cases (**Fig. 4a**). After incubation for 2 h at 37 °C, however, AP–neuroligin-1 labeled with wild-type streptavidin was strikingly clustered, whereas AP–neuroligin-1 labeled with monovalent streptavidin was still predominantly diffuse (**Fig. 4a**, **Supplementary Fig. 3** and **Supplementary Table 1** online). Wild-type streptavidin also promoted AP–neuroligin-1 clustering if cells were incubated with streptavidin for 24 h rather than 2 h (**Fig. 4b**).

We next examined the effect of AP–neuroligin-1 clustering on neuron function. To assess the formation of excitatory synapses by these neurons, we stained the cells with an antibody against the presynaptic marker vesicular glutamate transporter-1 (VGLUT1) (**Fig. 4b**). By itself, transfection with a transgene encoding hemagglutinin (HA)-tagged neuroligin-1 (HA–neuroligin-1) will increase the number and size of VGLUT1 clusters[15] (**Supplementary Table 2** online). Transfection with the transgene encoding AP–neuroligin-1 caused the same increase in VGLUT1 clusters as HA–neuroligin-1, if we added wild-type streptavidin just before fixation (so that there was no time for neuroligin clustering to occur). If we labeled biotinylated AP–neuroligin-1 with monovalent streptavidin for 24 h, we observed a similar increase in the number and intensity of VGLUT1 clusters as for HA–neuroligin-1. This suggests that the acceptor peptide tag, biotin and monovalent streptavidin do not interfere with the presynaptic differentiation promoted by neuroligin. But our preliminary observations showed that when biotinylated AP–neuroligin-1 was labeled with wild-type streptavidin for 24 h, this led to a reduction in VGLUT1 cluster intensity (**Fig. 4b** and **Supplementary Table 2**). In addition, the AP–neuroligin-1 clusters observed after treatment with wild-type streptavidin were often isolated rather than colocalized with VGLUT1 clusters (colocalization 49 ± 0.3 %; **Fig. 4b**). These results suggest that synapse formation can be disrupted by wild-type streptavidin labeling, a finding consistent with previous work indicating that artificial aggregation reduces the overall number of functional synapses formed[14,16]. The use of monovalent streptavidin, in contrast, can provide stable and specific labeling of neuroligin-1, without perturbing protein function through cross-linking.

DISCUSSION

We have generated a monovalent streptavidin, by making a chimeric streptavidin tetramer with a single active biotin binding subunit. This monovalent streptavidin bound to biotin with similar affinity and stability as wild-type streptavidin, did not rearrange its subunits over time and had high thermostability. Monovalent streptavidin should permit one to make use of its femtomolar binding affinity without additional unwanted multimerization.

Aside from illustrating how monovalent streptavidin can be used for stable and cross-linking–free protein detection in cellular imaging experiments, our experiments with neuroligin-1 demonstrate how engineered streptavidins can be used to examine the biological consequences of controlled clustering of cellular proteins. Cross-linking is used by cells to regulate protein activity, mobility and interactions, as demonstrated for many growth factor receptors and transcription factors[8]. Here we only compared monovalent and tetravalent (wild-type) streptavidins, but it would also be possible to use the entire series of purified streptavidin heterotetramers to examine the functional effects of receptor dimerization, trimerization and tetramerization.

The many alternative elegant approaches to site-specific labeling of proteins in living cells cannot all be described here, but have recently been reviewed[17–19]. The key point is that no single labeling approach is ideal in every circumstance. For example, fluorescent proteins or biarsenical labeling of tetracysteine tags[20] are valuable methods that do not suffer from probe dissociation or cause cross-linking, but they are limited for single-particle tracking by the moderate brightness and photobleaching of their fluorophores. Biarsenical labeling also cannot be used to label proteins specifically at the cell surface, although it has the advantage over our method that it can be used to label intracellular proteins. The advantages of labeling by means of site-specific biotinylation and monovalent streptavidin, as compared to antibody labeling, are twofold. First, the biotin-streptavidin interaction provides a much more stable linkage that permits long-term imaging over hours or even days. This strong interaction also eliminates the concern that the label might rapidly dissociate and reassociate with different cell-surface proteins over the time course of the imaging experiment, complicating tracking measurements. Second, antibodies are bivalent and can cross-link target proteins, as wild-type streptavidin does. Fab antibody fragments bind monovalently, but usually have substantially lower effective affinities, compounding the problem of antibody-epitope instability. Conversely, when high-affinity antibodies are available, antibodies have the advantage that they can be used to detect endogenous proteins, avoiding possible artifacts from transgene overexpression.

The need to purify different chimeric forms of streptavidin, as previously performed to improve reversibility[21,22] and as shown here, could be avoided if the four subunits could be genetically joined to make a single-chain streptavidin. But the large distance between the termini of streptavidin means that long linkers would be required, which are likely to impair folding. Attempts to circumvent this problem by circularly permuting streptavidin have yielded forms with $K_d > 10^{-8}$ M[23,24]. A circularly permuted tetravalent single-chain avidin with wild-type binding affinity was recently reported[25]. It will be valuable to generate an analogous single-chain tetravalent streptavidin and then to make it monovalent using the approach presented here, as avidin binds ~40-fold less tightly to biotin conjugates than streptavidin[26].

Bottom-up nanotechnology refers to the emerging use of self-assembly to construct multimolecular assemblies on the nanometer scale[27]. Streptavidin is one of the most common bridges in such assemblies, linking biotinylated DNA molecules, proteins and inorganic structures including carbon nanotubes and gold particles[27]. Such streptavidin bridges are either four-way junctions, if the biotinylated ligand is used at a saturating concentration, or statistical mixtures of zero- to four-way junctions, if the biotinylated ligand is used at a subsaturating concentration. The use of the chimeric streptavidin tetramers described in this paper should permit one to select whether a one-, two-, three- or four-way junction is generated. Poor yields of the desired junction, resulting from using a statistical mixture, are tolerable if there is only one step in assembly, but give unacceptable final yields if there are multiple steps in the assembly. This limits the complexity of the nanostructure that can be assembled. Thus chimeric streptavidins should be valuable building blocks for the construction of novel microarrayed sensors[28] and microelectronic circuits[29].

METHODS

Streptavidin expression and purification. We induced *E. coli* BL21(DE3) cells transformed with the streptavidin-pET21a expression plasmid (GenBank DQ376186), at OD_{600} 0.9 with 0.5 mM isopropyl-β-D-thiogalactopyranoside (IPTG). After incubating the cells for an additional 4 h at 37 °C, we purified inclusion bodies from the cell pellet using B-PER (Pierce), following manufacturer's instructions, and dissolved them in 6 M guanidinium hydrochloride (GuHCl; pH 1.5). To generate chimeric streptavidins, we estimated the concentration of each unfolded subunit from OD_{280} values in GuHCl and mixed the subunits in the desired ratio. We refolded the subunits in GuHCl by rapid dilution into PBS and concentrated them by ammonium sulfate precipitation, as described[30]. We redissolved the precipitate in PBS and dialyzed it 3× against PBS. This step was sufficient to purify A4, D4 and wild-type streptavidin. To purify chimeric streptavidins, we loaded a Poly-Prep column (Bio-Rad) with 1.8 ml Ni-NTA agarose (Qiagen) and washed it with 8 ml binding buffer (50 mM Tris-HCl, 300 mM NaCl; pH 7.8), using gravity flow at 26 °C. We diluted the streptavidin in PBS two-fold in binding buffer and loaded it onto the column. We washed the column with 8 ml washing buffer (binding buffer with 10 mM imidazole), eluting D4. Then we added 5 ml elution buffer 1 (binding buffer with 70 mM imidazole) and eluted A1D3, with some A2D2 eluted in later fractions. We collected 0.5-ml fractions of this elution, and of subsequent elutions with 5 ml elution buffer 2 (binding buffer with 100 mM imidazole), eluting principally A2D2, and then 5 ml elution buffer 3 (binding buffer with 125 mM imidazole), eluting principally A3D1. We mixed samples of each fraction with SDS loading buffer and then loaded the samples without boiling onto 8% SDS–polyacrylamide gels. We pooled and dialyzed fractions of the correct composition, determined by comparison to bands from the initial refold, in PBS. When required, we concentrated samples using a Centricon Ultracel YM10 (Millipore).

Cell culture, biotinylation and imaging. HeLa stably expressing AP-CFP-TM or Ala-CFP-TM have been previously described[7]. We prepared dissociated primary neuronal cultures from E18/19 rats and transfected them with transgenes encoding HA–neuroligin-1,

AP–neuroligin-1 or Ala–neuroligin-1 using Lipofectamine 2000 at division (DIV) 6 (ref. 15). All animal experiments were performed in accordance with the University of British Columbia Animal Care Committee.

We performed enzymatic biotinylation and imaging of HeLa transfectants as previously described[7], except instead of 10 μM biotin and 1 mM ATP, we added 10 μM biotin-AMP to give equivalent biotinylation (data not shown) while minimizing the risk of purinoreceptor activation by ATP. We biotinylated HeLa transfectants for 10 min at 26 °C, and stained with 10 μg/ml Alexa Fluor 568–conjugated wild-type streptavidin, D4 or A1D3 for 10 min at 4 °C. We biotinylated neurons at DIV 8 in Hanks' balanced salt solution (HBSS; Invitrogen) with 0.2 μM biotin ligase and 10 μM biotin-AMP for 5 min at 37 °C. We then washed neurons with HBSS and incubated for 2 min with 5 μg/ml Alexa Fluor 568–conjugated wild-type streptavidin (Molecular Probes) or A1D3 at 37 °C. After washing with NeuroBasal medium (Invitrogen) supplemented with 2% B-27 (Invitrogen), 50 U/ml penicillin, 50 μg/ml streptomycin and 0.2 mM L-glutamine, we incubated the neurons in the same medium for 0–2 h at 37 °C. Then we imaged the cells immediately or fixed them in –20 °C methanol. We did not observe labeling by wild-type streptavidin on neurons transfected with Ala–neuroligin-1 containing a point mutation in the acceptor peptide (data not shown), demonstrating the specificity of labeling[7].

To analyze excitatory synapses, we biotinylated the cells and stained them with streptavidin as above; we repeated biotinylation and streptavidin staining at 6 h, and incubated the cells for an additional 18 h before fixation in –20 °C methanol[15]. We stained samples for VGLUT1 using guinea pig anti-VGLUT1 (1:1,000; Chemicon) and then by goat anti-guinea pig Alexa Fluor 488 (1:1,000; Molecular Probes), both in blocking solution (PBS with 0.3% Triton X-100 and 2% normal goat serum; Vector Laboratories) for 1 h at 26 °C or overnight at 4 °C.

We collected images of HeLa cells on a Zeiss Axiovert 200M inverted epifluorescence microscope using a 40× oil-immersion lens and a MicroMAX charge-coupled device (CCD) camera (Roper Scientific). We collected CFP (420DF20 excitation, 450DRLP dichroic, 475DF40 emission) and Alexa Fluor 568 (560DF20 excitation, 585DRLP dichroic, 605DF30 emission) images and analyzed them using OpenLab software (Improvision). Fluorescence images were background-corrected. We acquired neuron images for 500–800 ms on a Zeiss Axiovert 200M microscope with a 63× 1.4 numerical aperture Acromat oil immersion lens and a monochrome 14-bit Zeiss Axiocam HR CCD camera with 1,300 × 1,030 pixels. In every case we prepared and imaged wild-type and A1D3 streptavidin samples under identical conditions. To correct for out-of-focus clusters within the field of view, we acquired focal-plane z stacks and performed maximum intensity projections off-line. Images were scaled to 16 bits and analyzed in Northern Eclipse (Empix Imaging) with user-written software. Briefly, images were processed at a constant threshold level (of 32,000 pixel values) to create a binary mask image, which was multiplied with the original image using Boolean image arithmetic. The resulting image contained a discrete number of clusters with pixel values of the original image. Only dendritic streptavidin clusters greater than 5 pixels in size and with an average pixel values two times greater than background pixel values were used for analysis. Results were then calculated in terms of clusters per micrometer of dendrite. For assessment of presynaptic termini, we used VGLUT1 clusters larger than 10 pixels for analysis, in which the average gray levels and number of clusters per micrometer were compared between transfected dendrites and untransfected dendrites within the same field of view. Colocalization of wild-type streptavidin clusters with VGLUT1 clusters was determined by Boolean image arithmetic from their binary mask images. Only clusters with a two-pixel overlap were counted as colocalization of pre- and postsynaptic termini. We performed the two-tailed parametric Student's *t*-test to calculate statistical significance of results between experimental groups. '*n*' represents the number of transfected neurons for which clusters were measured.

Additional methods. Descriptions of plasmid construction, fluorophore labeling of streptavidin, mass spectrometry and measurements of streptavidin K_d, off rate and thermostability are available in **Supplementary Methods**.

Note: Supplementary information is available on the Nature Methods website.

ACKNOWLEDGMENTS

Funding was provided by the National Institutes of Health (1 R01 GM072670-01), the EJLB foundation, the Dreyfus foundation, the Sloan foundation and the Massachusetts Institute of Technology. M.H. was supported by a Computational and Systems Biology Initiative MIT–Merck postdoctoral fellowship, D.J.-F.C. by a National Science and Engineering Research Council of Canada postdoctoral fellowship, K.G. by a Michael Smith Foundation for Health Research student fellowship, P.C.D. by a National Institutes of Health Kirschstein NRSA postdoctoral fellowship, N.L.K. by the National Institutes of Health, and A.E.-H. by the Canadian Institutes for Health Research, the Michael Smith Foundation for Health Research, Neuroscience Canada and EJLB foundation. We thank P. Stayton for the streptavidin plasmid, Tanabe USA for biotin, J.A. Ryan for assistance with synthesis and T.S. Chen for preparing AP–neuroligin-1 and Ala–neuroligin-1 constructs.

AUTHORS' CONTRIBUTIONS STATEMENT

M.H., D.J.-F.C., K.G. and P.C.D. performed the experiments. M.R.G. produced new reagents for the paper. M.H., A.E.-H., N.L.K. and A.Y.T. designed the research. M.H. and A.Y.T. wrote the paper.

COMPETING INTERESTS STATEMENT

The authors declare competing financial interests (see the *Nature Methods* website for details).

Published online at http://www.nature.com/naturemethods/
Reprints and permissions information is available online at http://npg.nature.com/reprintsandpermissions/

1. Green, N.M. Avidin and streptavidin. *Methods Enzymol.* **184**, 51–67 (1990).
2. Qureshi, M.H. & Wong, S.L. Design, production, and characterization of a monomeric streptavidin and its application for affinity purification of biotinylated proteins. *Protein Expr. Purif.* **25**, 409–415 (2002).
3. Laitinen, O.H. *et al.* Rational design of an active avidin monomer. *J. Biol. Chem.* **278**, 4010–4014 (2003).
4. Green, N.M. & Toms, E.J. The properties of subunits of avidin coupled to sepharose. *Biochem. J.* **133**, 687–700 (1973).
5. Sano, T. & Cantor, C.R. Intersubunit contacts made by tryptophan 120 with biotin are essential for both strong biotin binding and biotin-induced tighter subunit association of streptavidin. *Proc. Natl. Acad. Sci. USA* **92**, 3180–3184 (1995).
6. Chilkoti, A., Tan, P.H. & Stayton, P.S. Site-directed mutagenesis studies of the high-affinity streptavidin-biotin complex: contributions of tryptophan residues 79, 108, and 120. *Proc. Natl. Acad. Sci. USA* **92**, 1754–1758 (1995).
7. Howarth, M., Takao, K., Hayashi, Y. & Ting, A.Y. Targeting quantum dots to surface proteins in living cells with biotin ligase. *Proc. Natl. Acad. Sci. USA* **102**, 7583–7588 (2005).
8. Klemm, J.D., Schreiber, S.L. & Crabtree, G.R. Dimerization as a regulatory mechanism in signal transduction. *Annu. Rev. Immunol.* **16**, 569–592 (1998).

9. Klumb, L.A., Chu, V. & Stayton, P.S. Energetic roles of hydrogen bonds at the ureido oxygen binding pocket in the streptavidin-biotin complex. *Biochemistry* **37**, 7657–7663 (1998).
10. Reznik, G.O., Vajda, S., Sano, T. & Cantor, C.R. A streptavidin mutant with altered ligand-binding specificity. *Proc. Natl. Acad. Sci. USA* **95**, 13525–13530 (1998).
11. Hyre, D.E., Le, T.I., Freitag, S., Stenkamp, R.E. & Stayton, P.S. Ser45 plays an important role in managing both the equilibrium and transition state energetics of the streptavidin-biotin system. *Protein Sci.* **9**, 878–885 (2000).
12. Chen, I., Howarth, M., Lin, W. & Ting, A.Y. Site-specific labeling of cell surface proteins with biophysical probes using biotin ligase. *Nat. Methods* **2**, 99–104 (2005).
13. Scheiffele, P., Fan, J., Choih, J., Fetter, R. & Serafini, T. Neuroligin expressed in nonneuronal cells triggers presynaptic development in contacting axons. *Cell* **101**, 657–669 (2000).
14. Graf, E.R., Zhang, X., Jin, S.X., Linhoff, M.W. & Craig, A.M. Neurexins induce differentiation of GABA and glutamate postsynaptic specializations via neuroligins. *Cell* **119**, 1013–1026 (2004).
15. Prange, O., Wong, T.P., Gerrow, K., Wang, Y.T. & El Husseini, A. A balance between excitatory and inhibitory synapses is controlled by PSD-95 and neuroligin. *Proc. Natl. Acad. Sci. USA* **101**, 13915–13920 (2004).
16. Levinson, J.N. *et al.* Neuroligins mediate excitatory and inhibitory synapse formation: involvement of PSD-95 and neurexin-1β in neuroligin-induced synaptic specificity. *J. Biol. Chem.* **280**, 17312–17319 (2005).
17. Chen, I. & Ting, A.Y. Site-specific labeling of proteins with small molecules in live cells. *Curr. Opin. Biotechnol.* **16**, 35–40 (2005).
18. Johnsson, N., George, N. & Johnsson, K. Protein chemistry on the surface of living cells. *ChemBioChem* **6**, 47–52 (2005).
19. Miller, L.W. & Cornish, V.W. Selective chemical labeling of proteins in living cells. *Curr. Opin. Chem. Biol.* **9**, 56–61 (2005).
20. Griffin, B.A., Adams, S.R. & Tsien, R.Y. Specific covalent labeling of recombinant protein molecules inside live cells. *Science* **281**, 269–272 (1998).
21. Reznik, G.O., Vajda, S., Smith, C.L., Cantor, C.R. & Sano, T. Streptavidins with intersubunit crosslinks have enhanced stability. *Nat. Biotechnol.* **14**, 1007–1011 (1996).
22. Chilkoti, A., Schwartz, B.L., Smith, R.D., Long, C.J. & Stayton, P.S. Engineered chimeric streptavidin tetramers as novel tools for bioseparations and drug delivery. *Bio/Technology* **13**, 1198–1204 (1995).
23. Chu, V., Freitag, S., Le, T.I., Stenkamp, R.E. & Stayton, P.S. Thermodynamic and structural consequences of flexible loop deletion by circular permutation in the streptavidin-biotin system. *Protein Sci.* **7**, 848–859 (1998).
24. Aslan, F.M., Yu, Y., Mohr, S.C. & Cantor, C.R. Engineered single-chain dimeric streptavidins with an unexpected strong preference for biotin-4-fluorescein. *Proc. Natl. Acad. Sci. USA* **102**, 8507–8512 (2005).
25. Nordlund, H.R. *et al.* Tetravalent single chain avidin: From subunits to protein domains via circularly permuted avidins. *Biochem. J.* **392**, 485–491 (2005).
26. Nordlund, H.R., Hytonen, V.P., Laitinen, O.H. & Kulomaa, M.S. Novel avidin-like protein from a root nodule symbiotic bacterium, *Bradyrhizobium japonicum*. *J. Biol. Chem.* **280**, 13250–13255 (2005).
27. Niemeyer, C.M. Bioorganic applications of semisynthetic DNA-protein conjugates. *Chemistry* **7**, 3188–3195 (2001).
28. Wacker, R., Schroder, H. & Niemeyer, C.M. Performance of antibody microarrays fabricated by either DNA-directed immobilization, direct spotting, or streptavidin-biotin attachment: a comparative study. *Anal. Biochem.* **330**, 281–287 (2004).
29. Keren, K., Berman, R.S., Buchstab, E., Sivan, U. & Braun, E. DNA-templated carbon nanotube field-effect transistor. *Science* **302**, 1380–1382 (2003).
30. Schmidt, T.G. & Skerra, A. One-step affinity purification of bacterially produced proteins by means of the "Strep tag" and immobilized recombinant core streptavidin. *J. Chromatogr. A.* **676**, 337–345 (1994).

Targeting quantum dots to surface proteins in living cells with biotin ligase

Mark Howarth*, Keizo Takao†, Yasunori Hayashi†, and Alice Y. Ting*‡

*Department of Chemistry and †RIKEN-MIT Neuroscience Research Center, The Picower Center for Learning and Memory, Department of Brain and Cognitive Sciences, Massachusetts Institute of Technology, Cambridge, MA 02139

Communicated by Stephen J. Lippard, Massachusetts Institute of Technology, Cambridge, MA, April 15, 2005 (received for review February 28, 2005)

***Escherichia coli* biotin ligase site-specifically biotinylates a lysine side chain within a 15-amino acid acceptor peptide (AP) sequence. We show that mammalian cell surface proteins tagged with AP can be biotinylated by biotin ligase added to the medium, while endogenous proteins remain unmodified. The biotin group then serves as a handle for targeting streptavidin-conjugated quantum dots (QDs). This labeling method helps to address the two major deficiencies of antibody-based labeling, which is currently the most common method for targeting QDs to cells: the size of the QD conjugate after antibody attachment and the instability of many antibody–antigen interactions. To demonstrate the versatility of our method, we targeted QDs to cell surface cyan fluorescent protein and epidermal growth factor receptor in HeLa cells and to α-amino-3-hydroxy-5-methyl-4-isoxazolepropionate (AMPA) receptors in neurons. Labeling requires only 2 min, is extremely specific for the AP-tagged protein, and is highly sensitive. We performed time-lapse imaging of single QDs bound to AMPA receptors in neurons, and we compared the trafficking of different AMPA receptor subunits by using two-color pulse–chase labeling.**

BirA | labeling | streptavidin | glutamate receptor | single molecule

Quantum dots (QDs) are semiconductor nanoparticles that greatly expand the possibilities for fluorescence imaging of cells and living animals (1). Compared with small molecule dyes, the intense fluorescence emission of QDs makes it easier to track single protein molecules (2), they are remarkably resistant to photobleaching (3, 4), their narrow emission spectrum facilitates imaging of many proteins simultaneously (5), and their large two-photon cross sections allow *in vivo* imaging at greater depths (6). Since QDs have become commercially available, their use to study protein trafficking has grown rapidly. Two key problems we aimed to address in the use of QDs for tracking surface proteins are the size of the QD conjugate and dissociation of the QD from the protein of interest. The QDs themselves have a size comparable to GFP (Fig. 1*A*) (7). However, QDs are often targeted to the protein of interest with a three-layer strategy: primary antibody, followed by biotinylated secondary antibody, followed by streptavidin-QD (Fig. 1*A*). The size of this QD complex (≈50 nm) can affect membrane protein trafficking and can reduce accessibility to crowded locations in cells (8). Our aim was to develop a method to target QDs to cell surface proteins that eliminated the bulky antibodies and provided a stable linkage between the QD and the protein of interest.

Site-specific labeling of proteins in live cells poses an enormous challenge, because one must target the functional groups of one protein amidst all of the other expressed proteins containing the same range of amino acids. The merits and limitations of existing labeling approaches in cells have recently been reviewed (9). Here, we use the *Escherichia coli* enzyme biotin ligase (BirA) to address the challenge of specificity. BirA biotinylates a 15-amino acid peptide called the acceptor peptide (AP) (10, 11). BirA has previously been used to biotinylate AP-tagged proteins *in vitro* or when expressed in the cytosol (11, 12). BirA also biotinylates a truncated version of a bacterial transcarboxylase, when enzyme and substrate are coexpressed in the mammalian secretory pathway (13). The mammalian enzyme with biotin ligase activity, holocarboxylase synthetase (14), does not recognize AP as a substrate (12). In our approach for QD targeting (Fig. 1*B*), a cell surface protein fused to AP is biotinylated by adding recombinant BirA, ATP, and biotin to the medium. The biotinylated protein is then recognized by a streptavidin-conjugated QD. Biotin detection by streptavidin has numerous advantages. It is one of the tightest interactions known ($K_d = 10^{-13}$ M), with an off-rate on the order of days (15). In addition, streptavidin displays little nonspecific binding and is significantly smaller than an IgG antibody (60 versus 150 kDa), and a large number of streptavidin conjugates are commercially available. Nonspecific cell surface biotinylation is widely used to study membrane protein trafficking (16) and is commonly achieved by incubation of cells with an amine-reactive biotin probe. After lysis, surface proteins can be separated from internal proteins by using streptavidin-agarose. However, nonspecific biotinylation does not allow tracking of individual proteins by microscopy, and lysine residues important for protein function are sometimes modified (17).

α-Amino-3-hydroxy-5-methyl-4-isoxazolepropionate (AMPA) receptors are glutamate-activated ion channels and are tetramers composed of glutamate receptor (GluR) subunits 1–4 in various combinations. There is great interest in imaging AMPA receptors because their trafficking has a key role in modulating synaptic strength and thus learning and memory (18). We show first that BirA attaches biotin specifically to AP-tagged proteins on the surface of fibroblasts. We analyze the speed of this ligation and then show that this method allows QD targeting to specific cell surface proteins. We use BirA to label AMPA receptors in live neurons with QDs and examine the dynamics of the QD-labeled protein and how it colocalizes with synapses. The speed, specificity, and simplicity of labeling with BirA should make it a common tool for the study of cell surface proteins.

Materials and Methods

Bacterial Expression and Purification of BirA. BirA was purified and expressed as described in ref. 19. Briefly, His_6-tagged BirA was induced in *E. coli* JM109 and purified with Ni-nitrilotriacetic acid-agarose. Typical yields were 3 mg/liter of culture. BirA was stable for months in aliquots at −80°C. BirA copurifies with biotin-AMP. To perform appropriate negative controls, biotin-AMP was removed by incubating BirA with a substrate peptide, as described in ref. 19, to give "recycled" BirA. Recycled BirA was used in all experiments, except for that shown in Fig. 8, which is published as supporting information on the PNAS web site.

Freely available online through the PNAS open access option.

Abbreviations: QD, quantum dot; AP, acceptor peptide; AMPA, α-amino-3-hydroxy-5-methyl-4-isoxazolepropionate; GluR, glutamate receptor; CFP, cyan fluorescent protein; YFP, yellow fluorescent protein; PSD, postsynaptic density; TM, transmembrane; BirA, biotin ligase.

‡To whom correspondence should be addressed. E-mail: ating@mit.edu.

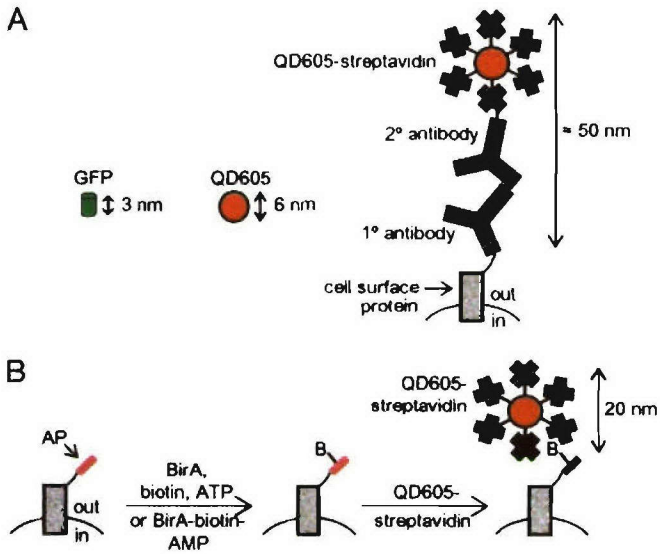

Fig. 1. General strategy for targeting QDs to cell surface proteins. (*A*) The size of GFP is compared with unconjugated QD605 and QD605-streptavidin conjugated to biotinylated secondary antibody and primary antibody, as used to label a cell surface protein. (*B*) The AP, GLNDIFEAQKIEWHE (shown in pink), is genetically encoded at the N terminus or C terminus of the protein of interest. Recombinantly expressed biotin ligase (BirA) is added to the cell medium with ATP and biotin, biotinylating AP. Excess biotin is removed by washing. Streptavidin-conjugated QDs are added to bind the biotinylated surface proteins. B, biotin.

Cell Surface Biotinylation. Cells were washed in PBS (pH 7.4) with 5 mM $MgCl_2$ (PBS-Mg), and biotinylation was performed in PBS-Mg with 0.3 μM BirA, 10 μM biotin, and 1 mM ATP for 1–60 min at room temperature. The cells were washed twice with PBS-Mg at 4°C and incubated with 10 μg/ml streptavidin-Alexa Fluor 568/Alexa Fluor 488 (Molecular Probes) or 10 nM streptavidin-QD605 (Quantum Dot, Hayward, CA) in PBS-Mg/1% predialyzed BSA for 10 min at 4°C. The cells were washed with PBS-Mg and imaged in the same buffer. Biotinylation was the same for neurons, except PBS-Mg was replaced with Tyrode's solution. For single-particle imaging, neurons were transfected 9 days after plating using calcium phosphate and imaged the next day. Cells were biotinylated for 5 min at 37°C, washed twice, and incubated with 0.4 nM streptavidin-QD605 for 2 min at room temperature. After one wash in Tyrode's solution and a second wash in Tyrode's solution with 10 μM biotin for 5 min, cells were imaged in a temperature-controlled chamber at 37°C. For myc staining, cells were stained with 4 μg/ml anti-myc antibody (Oncogene Science) in PBS-Mg/1% BSA for 30 min at 4°C. After two washes in PBS-Mg, cells were incubated in 20 μg/ml Alexa Fluor 568 anti-mouse IgG (Molecular Probes) in PBS-Mg/1% BSA for 30 min and then washed twice with PBS-Mg. All antibodies and streptavidin conjugates were centrifuged at 15,600 $\times$ *g* for 5 min at 4°C before use to remove aggregates.

Imaging. Images were collected on a Zeiss Axiovert 200M inverted epifluorescence microscope using a $\times$40 oil-immersion lens and a MicroMAX charge-coupled device camera (Roper Scientific, Trenton, NJ), except for Movie 1, which is published as supporting information on the PNAS web site, for which a 100$\times$ oil-immersion lens was used. Cyan fluorescent protein (CFP) (420DF20 excitation, 450DRLP dichroic, and 475DF40 emission), Alexa Fluor 568 (560DF20 excitation, 585 DRLP dichroic, and 605DF30 emission), QD605 (405 broad excitation, 585DRLP dichroic, and 605DF30 emission), yellow fluorescent protein (YFP) and Alexa Fluor 488 (495DF10 excitation, 515DRLP dichroic, and 530DF30 emission), and differential interference contrast images (630DF10 emission) were collected and analyzed with OPENLAB software (Improvision, Lexington, MA). Fluorescence images were background-corrected. Acquisition times ranged from 30 ms to 4 s. Movies were acquired with 0.1-s exposure and 0.3-s total delay between frames. Colocalization values were determined from the dendrites of four or more neurons by using OPENLAB: A region of interest was chosen surrounding a dendrite. Pixels were selected if they were >2 standard deviations above mean intensity. The percentage of colocalization for red or green pixels was calculated as the percentage of selected pixels of that color on which selected pixels of the other color superimposed. For each dendrite, both red and green percentage colocalizations were calculated, and the higher value was used. Means are given $\pm$SE, and significance was determined by using Student's *t* test.

Immunoblotting. After biotinylating as above, cells were washed in PBS and removed from the dish by scraping (trypsin could cleave AP). Cells were washed again in ice-cold PBS and kept at 4°C thereafter. Cells were lysed in 150 mM NaCl/5 mM EDTA/20 mM Tris·HCl/2 mM PMSF/1% protease inhibitor mixture (Calbiochem)/1% Triton X-100, pH 7.4 for 20 min. The postnuclear supernatant was mixed with an equal volume of 2$\times$ SDS/PAGE loading buffer with 5% 2-mercaptoethanol and run on a polyacrylamide gel. The number of cell equivalents loaded per lane was 1.5×10^5. After transfer to a nitrocellulose membrane, the membrane was blocked in Tris-buffered saline with 0.05% Tween 20 (TBST) and 3% BSA for 1 h. The membrane was incubated with 0.67 μg/ml ImmunoPure streptavidin-horseradish peroxidase (Pierce) in TBST for 40 min, washed four times for 5 min each time in TBST, developed in Supersignal West Pico substrate (Pierce), and imaged on a ChemiImager 5500 (Alpha Innotech, San Leandro, CA).

For further information on general materials, plasmid construction, and cell culture and transfection, see *Supporting Methods*, which is published as supporting information on the PNAS web site.

Results

Site-Specific Biotinylation of AP-Tagged Cell Surface Proteins. Our strategy for site-specific cell surface labeling is illustrated in Fig. 1*B*. Biotin ligase (BirA) is a 35-kDa protein that specifically biotinylates the 15-amino acid AP tag. We genetically attach AP to either terminus of the protein of interest and add recombinant BirA, ATP, and biotin to the cell medium. The population of biotinylated proteins at the surface is then detected with streptavidin-dye or a streptavidin-QD conjugate. Neither BirA nor streptavidin is membrane-permeable, so intracellular proteins are not labeled.

Initially, to demonstrate our method, we fused AP to CFP targeted to the surface with a signal peptide and the transmembrane (TM) domain of the platelet-derived growth factor receptor (AP-CFP-TM). We transfected this construct into HeLa cells. As a negative control, we made an equivalent construct with a point mutation at the acceptor lysine of AP (Ala-CFP-TM). BirA was added to the cell medium, along with ATP and biotin, and biotinylation was detected with streptavidin conjugated to Alexa Fluor 568 by fluorescence microscopy (Fig. 2). In the presence of BirA, ATP, and biotin, strong cell surface labeling with streptavidin was detected. The CFP signal serves as a control for equivalent expression of the protein target in each condition. A point mutation in AP, omitting BirA, or omitting biotin stopped all labeling. It is possible that other cell types would express endogenous substrates for BirA on their surfaces, diminishing the specificity of this labeling method. However, similar specificity was observed by fluorescence microscopy for

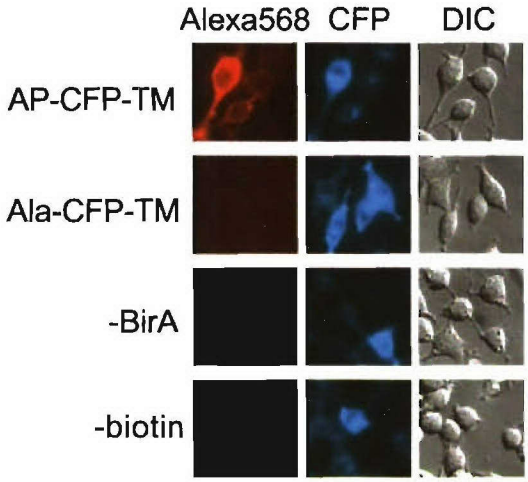

Fig. 2. Specific labeling of a cell surface protein by BirA shown by imaging. HeLa cells expressing AP-CFP-TM were biotinylated with BirA for 10 min. Biotinylated proteins at the cell surface were detected with streptavidin-Alexa Fluor 568. Controls are shown with a point mutation in AP (Ala-CFP-TM) or with BirA or biotin omitted from the labeling reaction.

AP-tagged proteins in human embryonic kidney (HEK) cells (data not shown), CHO cells (data not shown), and hippocampal neurons (see below).

We further tested the specificity of cell surface labeling with BirA by immunoblotting. HeLa cells transfected with AP-CFP-TM were incubated with BirA, ATP, and biotin. Total cell lysate was blotted with streptavidin-horseradish peroxidase (Fig. 3). Bands were detected in the absence of BirA because mammalian cells contain endogenous biotinylated proteins in the mitochondria and cytosol (14). However, there are no biotinylated proteins on the cell surface or in the secretory pathway. The only new biotinylated protein detected after incubation with BirA, ATP, and biotin corresponded to the molecular weight of AP-CFP-TM. Thus, BirA does not recognize endogenous proteins on the surface of HeLa cells, and AP-CFP-TM is not biotinylated by any endogenous enzyme. BirA labeling of AP-GluR2 showed similar specificity by immunoblotting in HeLa and HEK cells (data not shown).

We tested the sensitivity of this method of cell surface labeling by comparing it to antibody detection (Fig. 9, which is published as supporting information on the PNAS web site). AP-CFP-TM also has an extracellular myc tag. We compared the signal from myc to the signal from AP-CFP-TM biotinylation by using either

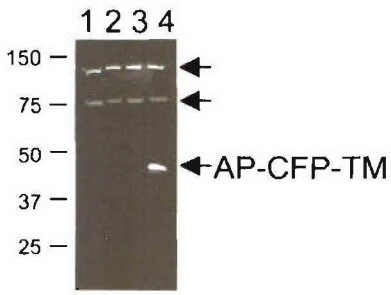

Fig. 3. Specific labeling of cell surface proteins by BirA shown by immunoblot. HeLa cells transfected with AP-CFP-TM were biotinylated with BirA for 5 min. Total cell lysates were blotted with streptavidin-horseradish peroxidase to detect biotinylated proteins. Results are shown for: lane 1, a point mutation in AP (Ala-CFP-TM); lane 2, without BirA; lane 3, without biotin; lane 4, with all components present. Endogenous biotinylated proteins are labeled with arrows and serve as a control for equivalent loading in each lane.

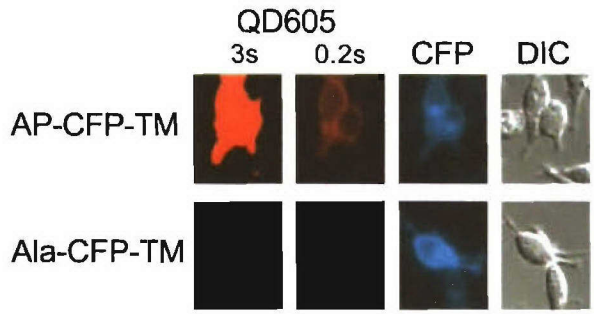

Fig. 4. QD labeling of cell surface proteins in HeLa cells. HeLa cells expressing AP-CFP-TM were biotinylated with BirA for 5 min. Biotinylation was detected with streptavidin-QD605. A control is shown with a point mutation in AP (Ala-CFP-TM). The QD605 signal is shown with 3-s and 0.2-s exposure.

anti-myc primary antibody followed by Alexa Fluor 568-conjugated secondary antibody or streptavidin-Alexa Fluor 568. When we normalized according to CFP intensity, the signal from biotinylation was ≈3-fold brighter than that from myc staining, showing that BirA labeling is a sensitive method for detecting cell surface proteins.

In many studies, it is useful to perform a pulse–chase, following the fate of proteins at various times after, for example, adding a drug or ligand. The shorter the pulse, the better the time resolution for the fate of the target protein. For this reason, we also determined the speed of BirA surface labeling on HeLa cells transfected with the AMPA receptor subunit AP-GluR2. We showed that labeling could be detected with streptavidin-Alexa Fluor 568 after only 1 min of incubation with BirA and was maximal at ≈10 min (Fig. 10, which is published as supporting information on the PNAS web site). We also found that cell surface biotinylation was comparably efficient in PBS with 5 mM $MgCl_2$, Hanks' balanced salt solution, DMEM, or DMEM with 10% FCS (data not shown).

Surface Protein Labeling with QDs. Having established the specificity of BirA for cell surface biotinylation, we determined whether streptavidin-conjugated QDs could be targeted to our protein of interest with similar specificity. The surface of QDs must be properly passivated to avoid nonspecific binding and consequent high backgrounds (1). The streptavidin-QD conjugates that we used in this study were passivated by the manufacturer using a proprietary mixed hydrophobic/philic polymer. HeLa cells expressing AP-CFP-TM were incubated briefly with BirA, and surface biotinylation was detected with streptavidin-QD605 and fluorescence microscopy (Fig. 4). A strong signal was detected on the surface of cells expressing AP-CFP-TM. Point mutation of AP or omitting BirA or biotin abolished the signal, and there was minimal background, even at long exposure times (3 s). Using a shorter exposure time of 0.2 s showed that the labeling was restricted to the cell surface. Thus, BirA provides an effective way to target QDs to cell surface proteins.

We compared the intensity of QD labeling to the brightest organic dyes, the Alexa Fluor series (20). Biotinylation was easily detectable with streptavidin-Alexa Fluor 568, but, as expected (21), the QD signal was much brighter and could be detected with a 30-fold shorter exposure time (Fig. 11*A*, which is published as supporting information on the PNAS web site). Thus, use of QD labeling would help to detect surface proteins with lower copy numbers. We also minimized the total time for QD labeling on the cell surface (Fig. 11*B*). Labeling was specific and clearly detectable after 2 min, showing that BirA can give good time resolution for tracking surface proteins with QDs.

To test the generality of this method for QD targeting, we attached AP to the epidermal growth factor receptor (EGFR).

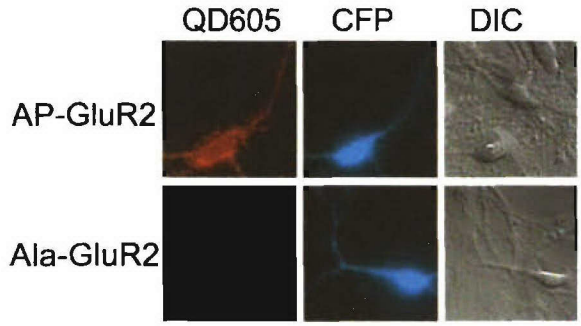

Fig. 5. Targeting QDs to AP-tagged AMPA receptors in neurons. Neurons transfected with AP-GluR2 were labeled with BirA for 5 min and then incubated with streptavidin-QD605. A control is shown with a point mutation in AP (Ala-GluR2). CFP was used as a cotransfection marker.

After incubating with BirA and streptavidin-QD605, AP-EGFR was clearly detected by fluorescence microscopy (Fig. 11*C*), whereas mutation of the acceptor lysine completely abolished labeling.

Site-Specific Targeting of QDs with BirA in Neurons. HeLa cells are robust to experimental manipulation, easy to transfect, and able to express recombinant proteins at high levels on the cell surface. Primary cells, specifically hippocampal neurons in dissociated culture, pose a more challenging test of our labeling method and allow us to determine whether we can use BirA as a tool for analyzing the dynamics of AMPA receptor trafficking.

Hippocampal neurons were transfected with AP-GluR2 and incubated with BirA. Streptavidin-conjugated QDs were then used to detect surface biotinylation (Fig. 5). QD fluorescence was clearly detected on cells expressing AP-GluR2, indicated by the presence of the cotransfection marker CFP, but not on untransfected cells. The signal was abolished by point mutation of AP (Fig. 5) or by omitting BirA or biotin (data not shown). It is unlikely that AP would disrupt the function of the AMPA receptor because fusion at the same site to the much larger GFP did not change localization, interaction with other subunits, or electrophysiological properties of GluR1 (22) or GluR2 (23). Thus, BirA allows cell surface labeling of AP-tagged proteins but does not label endogenous proteins in neurons, which should allow our method to be used for studies of neurotransmitter receptor trafficking.

Effect of the QD Label on AMPA Receptor Localization. QDs greatly facilitate single-molecule tracking of cell surface proteins, which gives crucial information on internalization, diffusion, and the presence of membrane domains. However, there is some concern that the size of the QD reduces movement of attached proteins. For our method, we wanted to test (*i*) whether streptavidin-QDs could bind to biotinylated AP-GluR2 at the synapse and (*ii*) whether we could detect any difference in the distribution of AP-GluR2, when it is detected with streptavidin-QD versus streptavidin conjugated to the much smaller Alexa Fluor dyes.

Hippocampal neurons were cotransfected with AP-GluR2 and the synaptic marker postsynaptic density (PSD)-95 fused to YFP (24). After incubating with BirA, cells were labeled with streptavidin-QD605 (Fig. 6*A*). The colocalization between streptavidin-QD605 and PSD-95-YFP was moderate at 70 ± 3%. QD staining was visible at some PSD-95-YFP puncta, suggesting that the size of the QD does not eliminate synaptic localization. However, there were many regions with only QD or only PSD-95-YFP staining. The specificity of the QD staining was demonstrated by using cells transfected with Ala-GluR2 (data not shown). To determine whether this nonsynaptic staining of

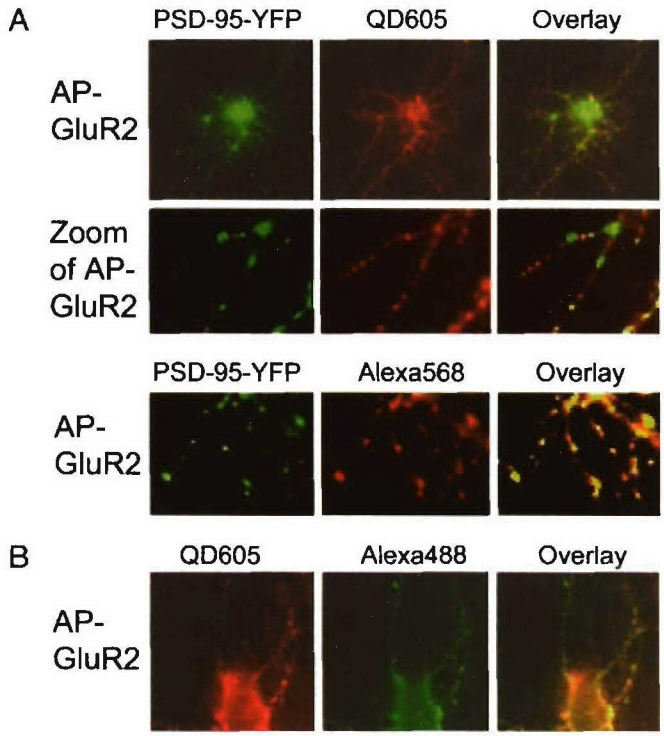

Fig. 6. The effect of QD size on surface labeling in neurons. (*A*) Neurons expressing AP-GluR2 and the synaptic marker PSD-95-YFP were labeled with BirA for 10 min at 37°C. After biotinylation, neurons were stained with streptavidin-QD605. (*Middle*) The staining at higher zoom. (*Bottom*) The same experiment, except the biotinylation was detected with streptavidin-Alexa Fluor 568 instead of streptavidin-QD605. (*B*) Neurons expressing AP-GluR2 were labeled with BirA for 10 min at 37°C. They were then incubated simultaneously with streptavidin-Alexa Fluor 488 and streptavidin-QD605.

GluR2 was caused by AP (without the QD attachment), we repeated the experiment but detected biotinylation of AP-GluR2 with the smaller probe streptavidin-Alexa Fluor 568 (Fig. 6*A*). In this case, the degree of overlap between streptavidin-Alexa Fluor 568 and PSD-95-YFP was significantly greater (80 ± 3%; $P < 0.05$), with streptavidin-Alexa Fluor 568 staining visible at nearly all PSD-95-YFP puncta. This difference in colocalization indicates that some synaptic AP-GluR2 molecules are not accessible to streptavidin-QD605, most likely because of QD size.

To further investigate this, we also transfected neurons with AP-GluR2 alone. Then, after site-specific biotinylation, streptavidin-QD605 and streptavidin-Alexa Fluor 488 were allowed to compete for binding to biotinylated AP-GluR2 (Fig. 6*B*). The QD signal and Alexa Fluor 488 signal overlapped at many places but were distinct in other places (colocalization = 58 ± 3%), indicating that QD size can affect streptavidin recognition of certain AP-GluR2 subpopulations.

Analysis of AMPA Receptor Trafficking by Using Two-Color Pulse–Chase Labeling. To map the changing distribution of a cell surface protein with BirA, we incubated the tagged AMPA receptor subunits AP-GluR1 or AP-GluR2 at the neuron surface with BirA and briefly labeled with streptavidin-Alexa Fluor 488. We then added glycine to stimulate activation-induced remodeling of the neuronal surface (25). The cells were labeled a second time with BirA, and this population was detected with streptavidin-QD605 (Fig. 7). Labeling of AP-GluR1 was barely detectable in the basal state, but a good signal was observed after glycine stimulation. Ala-GluR1 did not give any signal under the same

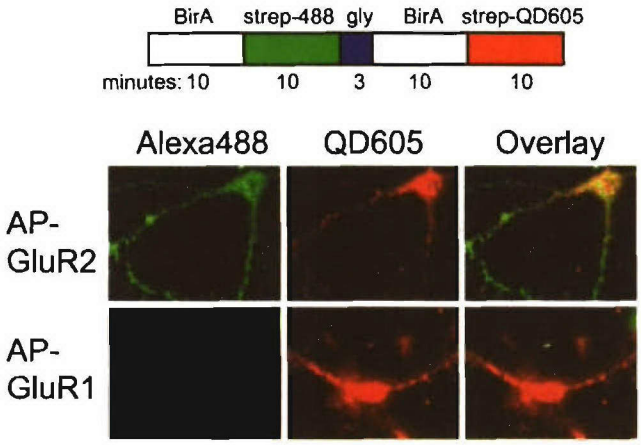

Fig. 7. Pulse–chase labeling of AMPA receptor subunits. Neurons were transfected with AP-GluR1 or AP-GluR2 and labeled with BirA for 10 min at 37°C followed by streptavidin-Alexa Fluor 488 for 10 min at room temperature. After 3 min at room temperature with 200 μM glycine, the neurons were again incubated with BirA for 10 min at 37°C and streptavidin-QD605 for 10 min at 4°C before imaging.

conditions (data not shown). In contrast, AP-GluR2 gave a good signal in the basal state, and the signal was little affected by glycine treatment, in agreement with the results of Passafaro *et al.* (26).

Single-Particle Imaging of QDs Bound to Neuronal Proteins. We made use of the photophysical properties of QDs to track the movements of single AP-tagged AMPA receptors in neurons. We cotransfected hippocampal neurons with AP-GluR2 and PSD-95-YFP. After brief incubation with BirA and then streptavidin-QD605 (at 25-fold lower concentration than for Figs. 5–7), we imaged the dynamics of QD-labeled AP-GluR2 proteins (Movie 1). We were able to detect single QDs bound to the neurons, as determined by comparison to the intensity of diluted QDs spread on a glass slide (data not shown) and by the QD blinking behavior (27) (particles whose fluorescence completely disappears and then abruptly reappears, as plotted in Fig. 12, which is published as supporting information on the PNAS web site). A proportion of AP-GluR2 molecules showed rapid movement to and from regions that were largely immobile. Low mobility may reflect tethering to scaffold proteins or endocytosis of the QD bound to AP-GluR2 (28). We observed stable signals at PSD-95-YFP puncta (two examples are marked with arrows), but it is possible that other immobile spots also represent synapses that could be resolved with Mitotracker labeling (8).

Discussion

We have developed a general method to target QDs to cell surface proteins. Biotin ligase (BirA) specifically recognizes proteins bearing an AP at the cell surface, as demonstrated by fluorescence microscopy and immunoblotting. Biotinylated proteins at the cell surface can then be detected by streptavidin-conjugated QDs. We demonstrated this method for surface-displayed CFP and the epidermal growth factor receptor in HeLa cells and for GluR1 and GluR2 in neurons. Because biotinylation can be detected after 1 min, this method has the potential to give precise time resolution for studies of cell surface trafficking. The small size of AP means that it is unlikely to perturb folding, secretion, and protein–protein interactions during trafficking to the surface, compared with fluorescent proteins (GFP is 238 residues) (29, 30) or other proteins directing site-specific labeling, such as O^6-alkylguanine-DNA alkyltransferase (31) or acyl carrier protein (32).

A key advantage of QDs is their photostability, which allows imaging over much longer periods than organic dyes. However, if cells are to be imaged over periods of hours to days, it is of no use if the QD has already detached from the protein of interest. Thus, the stability of streptavidin–biotin interaction in our system may help to realize the potential of QDs for long-term imaging. Also, using biotin to direct QD labeling significantly reduces the size of the QD conjugate compared with two- or three-layer antibody targeting. Using biotin ligase targeting will reduce the steric hindrance of the QD conjugate that may restrict access to certain regions of the cell surface or impair endocytosis. Fab antibody fragments could be used instead to reduce the size of QD antibody conjugates, but they tend to dissociate rapidly from their target protein. We biotinylated the AMPA receptor subunit GluR2 tagged with AP on neurons and tested the colocalization with a synaptic marker. QD fluorescence was present at many synapses, but the degree of colocalization was less than when AP-GluR2 was detected with streptavidin-Alexa Fluor 488. Similarly, when neurons expressing AP-GluR2 were biotinylated and coincubated with streptavidin-Alexa Fluor 488 and streptavidin-QD, there was only partial overlap between the Alexa Fluor 568 and QD signal. Thus, even though we have reduced the size of the QD conjugate compared with previous studies (8), the QD may still restrict access to certain parts of the cell surface. Because QDs can themselves be detected on the electron microscope (33), analysis of QD-labeled neurons by electron microscopy should allow us to address at greater resolution the question of access to synapses (2).

One concern common to targeting QDs with antibodies, streptavidin, or receptor ligands is the difficulty of attaching a single binding unit to the QD, which means that it is possible for the QD to cross-link cell surface proteins and thus disrupt their function. Using an excess of QD over the protein target helps to promote monovalent binding and minimize cross-linking. Derivatizing the QD surface with a single streptavidin protein and using monomeric rather than tetrameric streptavidin (34) could eliminate this concern. Also, an apprehension regarding the use of BirA for surface labeling is the presence of ATP in the labeling medium, because ATP and its degradation products can activate signaling pathways (35). However, recombinant BirA copurifies with biotin-AMP in the active site ($K_d = 10^{-10}$ M) (36), and we have shown that the BirA–biotin–AMP complex can efficiently label AP-tagged proteins without addition of ATP to cells (Fig. 8).

Apart from its use in targeting QDs, BirA labeling of surface proteins could become a general method for analyzing protein–protein interactions and trafficking of cell surface proteins. For example, BirA can label proteins with ^{3}H biotin (data not shown), or streptavidin could be used for immunoprecipitation, immunoblotting, or flow cytometry of surface proteins biotinylated with BirA. The advantages over genetically encoded tags for antibody recognition, such as myc or hemagglutinin, are two-fold. First, one can pulse-label a cohort of surface molecules with BirA, and the chase can be conducted with the protein modified only by the addition of a biotin group (0.24 kDa) rather than an antibody (150 kDa), so there will be less perturbation of protein interactions and trafficking. The biotin group can then be detected with streptavidin after the chase is over. Second, the remarkable stability of biotin-streptavidin binding enables more sensitive and stable detection and allows more stringent washing for purification, which improves the signal-to-noise ratio (37–39). However, antibodies to endogenous proteins, when available, do avoid the concern of the effect of overexpression when observing the behavior of transfected proteins.

The movement of AMPA receptors in the plasma membrane is important for synaptic plasticity, because both diffusion from extrasynaptic sites and exocytosis of AMPA receptors strengthen synapses (28). Our initial studies tracking GluR2 dynamics using

BirA and QD labeling showed that we could detect single QDs, even using lamp rather than laser excitation. The mobility of AP-GluR2 is dramatic (8). BirA targeting of QDs could be used to investigate what factors control this mobility, and observations could be extended to GluR1 and GluR3. AMPA receptor trafficking has been analyzed with other labeling approaches (26, 40, 41). For example, fusion of GFP to GluR1 showed activity-dependent movement into dendritic spines (22), but pH-sensitive GFP was required to distinguish GluR1 in vesicles near the cell surface from GluR1 inserted into the postsynaptic membrane (41). The moderate brightness and multiple dark states of fluorescent proteins, however, make them poor for single particle imaging. AMPA receptors have also been tagged with a tetracysteine motif and observed with FlAsH, a fluorescent arsenical probe (42). However, FlAsH is not suitable for cell surface labeling, because it requires reduction of cell surface thiols, and the labeling protocol requires an hour, so rapid events cannot be detected. Biotin ligase labeling provides a specific, rapid, and generally applicable method for detecting and tracking cell surface proteins.

We thank Tanabe U.S.A. (San Diego) for biotin; I. Chen, E. Njie, J. Baskin, B. Schneider, C.-W. Lin, and H. Ames for assistance; and M. Bawendi, S. S. Licht, and R. Y. Tsien for helpful advice. This paper is dedicated to A. D. B. Arnold. This work was supported by National Institutes of Health Grants K22-HG002671-01 and 1 P20GM072029-01, the EJLB Foundation, Massachusetts Institute of Technology (MIT), a Computational and Systems Biology Initiative MIT-Merck Postdoctoral Fellowship (to M.H.), a Special Postdoctoral Researchers Fellowship from RIKEN (to K.T.), and The Ellison Medical Foundation (Y.H.).

1. Gao, X., Yang, L., Petros, J. A., Marshall, F. F., Simons, J. W. & Nie, S. (2005) *Curr. Opin. Biotechnol.* **16,** 63–72.
2. Dahan, M., Levi, S., Luccardini, C., Rostaing, P., Riveau, B. & Triller, A. (2003) *Science* **302,** 442–445.
3. Chan, W. C. & Nie, S. (1998) *Science* **281,** 2016–2018.
4. Bruchez, M., Jr., Moronne, M., Gin, P., Weiss, S. & Alivisatos, A. P. (1998) *Science* **281,** 2013–2016.
5. Han, M., Gao, X., Su, J. Z. & Nie, S. (2001) *Nat. Biotechnol.* **19,** 631–635.
6. Larson, D. R., Zipfel, W. R., Williams, R. M., Clark, S. W., Bruchez, M. P., Wise, F. W. & Webb, W. W. (2003) *Science* **300,** 1434–1436.
7. Jaiswal, J. K. & Simon, S. M. (2004) *Trends Cell Biol.* **14,** 497–504.
8. Groc, L., Heine, M., Cognet, L., Brickley, K., Stephenson, F. A., Lounis, B. & Choquet, D. (2004) *Nat. Neurosci.* **7,** 695–696.
9. Chen, I. & Ting, A. Y. (2005) *Curr. Opin. Biotechnol.* **16,** 35–40.
10. Schatz, P. J. (1993) *Biotechnology (N.Y.)* **11,** 1138–1143.
11. Beckett, D., Kovaleva, E. & Schatz, P. J. (1999) *Protein Sci.* **8,** 921–929.
12. de Boer, E., Rodriguez, P., Bonte, E., Krijgsveld, J., Katsantoni, E., Heck, A., Grosveld, F. & Strouboulis, J. (2003) *Proc. Natl. Acad. Sci. USA* **100,** 7480–7485.
13. Parrott, M. B. & Barry, M. A. (2001) *Biochem. Biophys. Res. Commun.* **281,** 993–1000.
14. Chapman-Smith, A. & Cronan, J. E., Jr. (1999) *Biomol. Eng.* **16,** 119–125.
15. Piran, U. & Riordan, W. J. (1990) *J. Immunol. Methods* **133,** 141–143.
16. Hurley, W. L., Finkelstein, E. & Holst, B. D. (1985) *J. Immunol. Methods* **85,** 195–202.
17. Gite, S., Reddy, G. & Shankar, V. (1992) *Biochem. J.* **285,** Part 2, 489–494.
18. Malinow, R. & Malenka, R. C. (2002) *Annu. Rev. Neurosci.* **25,** 103–126.
19. Chen, I., Howarth, M., Lin, W. & Ting, A. Y. (2005) *Nat. Methods* **2,** 99–104.
20. Panchuk-Voloshina, N., Haugland, R. P., Bishop-Stewart, J., Bhalgat, M. K., Millard, P. J., Mao, F., Leung, W.-Y. & Haugland, R. P. (1999) *J. Histochem. Cytochem.* **47,** 1179–1188.
21. Wu, X., Liu, H., Liu, J., Haley, K. N., Treadway, J. A., Larson, J. P., Ge, N., Peale, F. & Bruchez, M. P. (2003) *Nat. Biotechnol.* **21,** 41–46.
22. Shi, S. H., Hayashi, Y., Petralia, R. S., Zaman, S. H., Wenthold, R. J., Svoboda, K. & Malinow, R. (1999) *Science* **284,** 1811–1816.
23. Shi, S., Hayashi, Y., Esteban, J. A. & Malinow, R. (2001) *Cell* **105,** 331–343.
24. Craven, S. E., El Husseini, A. E. & Bredt, D. S. (1999) *Neuron* **22,** 497–509.
25. Lu, W., Man, H., Ju, W., Trimble, W. S., MacDonald, J. F. & Wang, Y. T. (2001) *Neuron* **29,** 243–254.
26. Passafaro, M., Piech, V. & Sheng, M. (2001) *Nat. Neurosci.* **4,** 917–926.
27. Nirmal, M., Dabbousi, B. O., Bawendi, M. G., Macklin, J. J., Trautman, J. K., Harris, T. D. & Brus, L. E. (1996) *Nature* **383,** 802–804.
28. Choquet, D. & Triller, A. (2003) *Nat. Rev. Neurosci.* **4,** 251–265.
29. Lisenbee, C. S., Karnik, S. K. & Trelease, R. N. (2003) *Traffic* **4,** 491–501.
30. Huh, W. K., Falvo, J. V., Gerke, L. C., Carroll, A. S., Howson, R. W., Weissman, J. S. & O'Shea, E. K. (2003) *Nature* **425,** 686–691.
31. Keppler, A., Gendreizig, S., Gronemeyer, T., Pick, H., Vogel, H. & Johnsson, K. (2003) *Nat. Biotechnol.* **21,** 86–89.
32. George, N., Pick, H., Vogel, H., Johnsson, N. & Johnsson, K. (2004) *J. Am. Chem. Soc.* **126,** 8896–8897.
33. Nisman, R., Dellaire, G., Ren, Y., Li, R. & Bazett-Jones, D. P. (2004) *J. Histochem. Cytochem.* **52,** 13–18.
34. Wu, S. C. & Wong, S. L. (2004) *Anal. Biochem.* **331,** 340–348.
35. Rathbone, M. P., Middlemiss, P. J., Gysbers, J. W., Andrew, C., Herman, M. A., Reed, J. K., Ciccarelli, R., Di Iorio, P. & Caciagli, F. (1999) *Prog. Neurobiol.* **59,** 663–690.
36. Xu, Y. & Beckett, D. (1994) *Biochemistry* **33,** 7354–7360.
37. Viens, A., Mechold, U., Lehrmann, H., Harel-Bellan, A. & Ogryzko, V. (2004) *Anal. Biochem.* **325,** 68–76.
38. Penalva, L. O. & Keene, J. D. (2004) *BioTechniques* **37,** 604, 606, 608–610.
39. Tucker, J. & Grisshammer, R. (1996) *Biochem. J.* **317,** Part 3, 891–899.
40. Sekine-Aizawa, Y. & Huganir, R. L. (2004) *Proc. Natl. Acad. Sci. USA* **101,** 17114–17119.
41. Ashby, M. C., De la Rue, S. A., Ralph, G. S., Uney, J., Collingridge, G. L. & Henley, J. M. (2004) *J. Neurosci.* **24,** 5172–5176.
42. Ju, W., Morishita, W., Tsui, J., Gaietta, G., Deerinck, T. J., Adams, S. R., Garner, C. C., Tsien, R. Y., Ellisman, M. H. & Malenka, R. C. (2004) *Nat. Neurosci.* **7,** 244–253.

Site-specific labeling of cell surface proteins with biophysical probes using biotin ligase

Irwin Chen, Mark Howarth, Weiying Lin & Alice Y Ting

We report a highly specific, robust and rapid new method for labeling cell surface proteins with biophysical probes. The method uses the *Escherichia coli* enzyme biotin ligase (BirA), which sequence-specifically ligates biotin to a 15-amino-acid acceptor peptide (AP). We report that BirA also accepts a ketone isostere of biotin as a cofactor, ligating this probe to the AP with similar kinetics and retaining the high substrate specificity of the native reaction. Because ketones are absent from native cell surfaces, AP-fused recombinant cell surface proteins can be tagged with the ketone probe and then specifically conjugated to hydrazide- or hydroxylamine-functionalized molecules. We demonstrate this two-stage protein labeling methodology on purified protein, in the context of mammalian cell lysate, and on epidermal growth factor receptor (EGFR) expressed on the surface of live HeLa cells. Both fluorescein and a benzophenone photoaffinity probe are incorporated, with total labeling times as short as 20 min.

Biophysical probes such as fluorophores, photoaffinity labels and spin labels have been extremely useful for investigating protein structure and function *in vitro*, but technological hurdles have limited their use in the heterogeneous context of the cytoplasm or cell surface. Green fluorescent protein (GFP) is an attractive option because of its high labeling specificity and ease of use, but it is a large tag (238 amino acids) and can be used only for fluorescence imaging. Recent protein-based tags that either react covalently or form high-affinity complexes with small-molecule probes circumvent the problem of versatility, as in principle probes of any structure can be introduced, but the problem of size remains[1–5]. In addition, tags based on endogenous mammalian proteins such as O^6-alkylguanine transferase (AGT) and dihydrofolate reductase (DHFR) produce background labeling of their endogenous counterparts in mammalian cells[1,2]. In addition, the noncovalent interactions on which DHFR and FK506 binding protein (FKBP) labeling rely dissociate over minutes to hours, causing signal deterioration[2,3].

Labeling approaches that use peptides rather than proteins as targeting sequences are less invasive but generally sacrifice specificity. For instance, the FlAsH technology, which targets arsenic-functionalized fluorophores to tetracysteine motifs displayed on recombinant proteins, requires complex washout procedures to remove the probe from monothiols inside cells[6]. Fluorophore-binding peptide aptamers similarly show reduced specificity compared to protein tag–based methods[7]. The recently developed hexahistidine-based labeling approach may offer higher specificity but also relies on a noncovalent interaction that deteriorates within minutes[8]. We have recently reviewed the merits and disadvantages of existing labeling methodologies elsewhere[9].

Thus, there is a need for new methodology that combines the minimal invasiveness of a small peptide tag with the excellent labeling specificity of GFP. Moreover, the attachment strategy should be covalent, so that probe dissociation is not a concern. To address this problem, we capitalized on the *E. coli* enzyme BirA, which catalyzes the biotinylation of a lysine side-chain within a 15-amino-acid consensus 'acceptor peptide' (AP) sequence[10]. BirA has already been used for the specific biotinylation of AP-fused recombinant proteins *in vitro* and in living cells, because of its excellent sequence specificity; endogenous mammalian proteins are not modified by BirA[11], and bacteria have only one natural substrate, biotin carboxyl carrier protein (BCCP)[10]. The mechanism of biotinylation involves activation of biotin as an adenylate ester, followed by its trapping by the lysine side-chain of the AP. To harness the specificity of BirA for ligation of other biophysical probes to proteins, we sought to re-engineer the biotin binding site to accommodate various biotin analogs. We were particularly interested in ketone 1, a biotin isostere with the ureido nitrogens replaced by methylene groups (**Fig. 1a**). Because the ketone group is absent from natural proteins, carbohydrates and lipids, it can be selectively derivatized on cell surfaces with hydrazide- or hydroxylamine-bearing probes under physiological conditions[12]. Here we describe the development of new protein labeling methodology (**Fig. 1**) based on the observation that wild-type BirA uses ketone 1 efficiently in place of biotin.

RESULTS

Wild-type BirA ligates ketone 1 to the AP

Racemic ketone 1 was synthesized in four steps from a known sulfoxide[13] in a route that recapitulates one of the known syntheses of biotin (**Fig. 1b** and **Supplementary Methods** online)[14]. We developed an HPLC-based assay to determine whether wild-type or

Department of Chemistry, Massachusetts Institute of Technology, 77 Massachusetts Ave., Room 18-496, Cambridge, Massachusetts 02139, USA. Correspondence should be addressed to A.Y.T. (ating@mit.edu).

PUBLISHED ONLINE 21 JANUARY 2005; DOI:10.1038/NMETH735

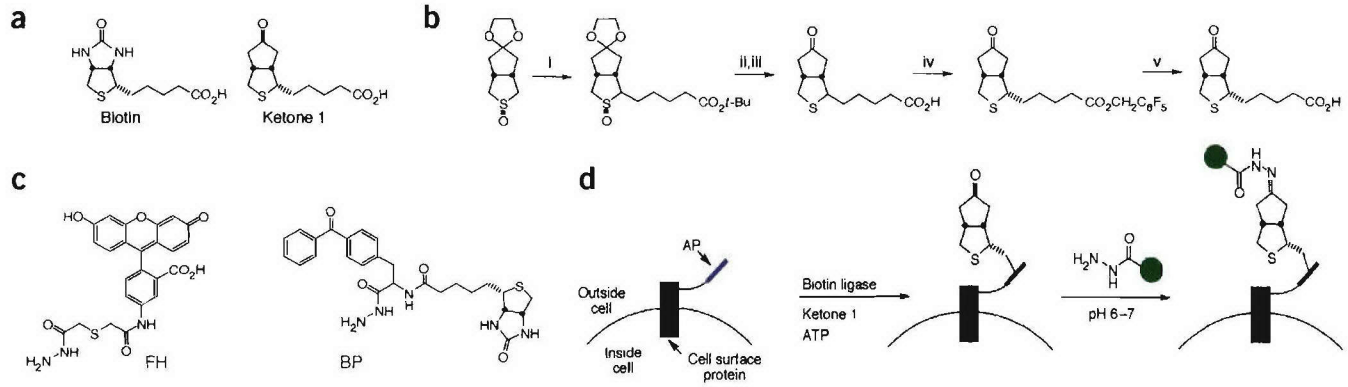

Figure 1 | Site-specific protein labeling using biotin ligase and a ketone analog of biotin. (**a**) Structures of biotin and ketone 1. (**b**) Synthesis of ketone 1. **i.** MeLi, THF/HMPA, −78 °C, then $I(CH_2)_4CO_2t$-Bu, −30 °C. **ii.** PPh_3, CCl_4, reflux. **iii.** AcOH, aq. HCl, reflux. **iv.** DIPEA, $C_6F_5CH_2Br$, CH_2Cl_2, then HPLC separation of diastereomers. **v.** LiOH, THF/MeOH/H_2O. (**c**) Structures of fluorescein hydrazide (FH) and benzophenone-biotin hydrazide (BP). (**d**) General method for labeling acceptor peptide (AP)-tagged recombinant cell surface proteins with biophysical probes. Biotin ligase (BirA) catalyzes the ligation of ketone 1 to the AP (blue); a subsequent bio-orthogonal ligation between ketone and hydrazide (or hydroxylamine) introduces the probe (green).

a mutant of BirA could catalyze the ligation of this probe to a synthetic acceptor peptide. When we combined wild-type BirA with synthetic AP, ketone 1, and ATP, a new product peak was observed by HPLC; omission of ATP or BirA from the reaction eliminated this peak (**Fig. 2a**). MALDI-TOF analysis confirmed that the product had the expected molecular weight for ketone 1 ligated to the AP (calculated (plus sodium ion) 2,541.3 g/mol; observed 2,542.3 g/mol) (**Fig. 2b**). Ketone 1 was also separated into its constituent enantiomers by chiral HPLC, and we verified that only one enantiomer was accepted by BirA (data not shown).

To quantitatively compare the rate of BirA-catalyzed ketone 1 ligation to that of biotin ligation, we measured the rates of product formation for both reactions under identical conditions (**Fig. 2c**). The initial rate for ketone 1 ligation (0.258 ± 0.024 μM/min) was lower by only a factor of 3.7 than that for biotin ligation (0.954 ± 0.018 μM/min, matching the previously reported rate for BirA biotinylation of BCCP[15]). However, whereas the biotin ligation rate remained constant until >50% conversion, the ketone ligation rate slowed markedly after ~100 enzyme turnovers, suggesting that product inhibition might be occurring. To avoid such inhibition, we used >0.01 equivalents of BirA relative to protein substrate in all subsequent labeling experiments.

In vitro labeling of recombinant proteins

To test the use of BirA and ketone 1 for labeling of a recombinant protein, we generated a test substrate by fusing the AP to the C terminus of cyan fluorescent protein (CFP-AP). Purified CFP-AP was first enzymatically labeled with ketone 1, and then fluorescein hydrazide was added to derivatize the ketone. The resulting hydrazone adduct was reduced with sodium cyanoborohydride to improve its stability and separated from excess fluorophore by SDS-PAGE. The fluorescence and Coomassie blue–stained images of the resulting gel are shown (**Figs. 3a,b**). Fluorescein is conjugated to CFP-AP only when ATP is present in the enzymatic ligation reaction, indicating that conjugation is dependent on enzyme activity. Point mutation of the CFP-AP acceptor lysine to alanine (CFP-Ala) also abolishes fluorescein conjugation, demonstrating that the labeling is site specific.

To test the specificity of the BirA-mediated labeling reaction, we expressed CFP-AP in human embryonic kidney 293T (HEK) cells and then subjected the cellular lysate to the same two-stage labeling procedure used before (**Figs. 3c,d**). Only CFP-AP is labeled with fluorescein, even in the presence of endogenous mammalian proteins at similar concentration. Again, labeling is dependent on the presence of ATP, and lysates from untransfected HEK cells are not labeled. Thus, wild-type BirA accepts ketone 1 as a cofactor without compromising its exceptional specificity for the peptide substrate.

We also assessed the sensitivity of our labeling method by comparing it to antibody detection. Lysate from CFP-AP-

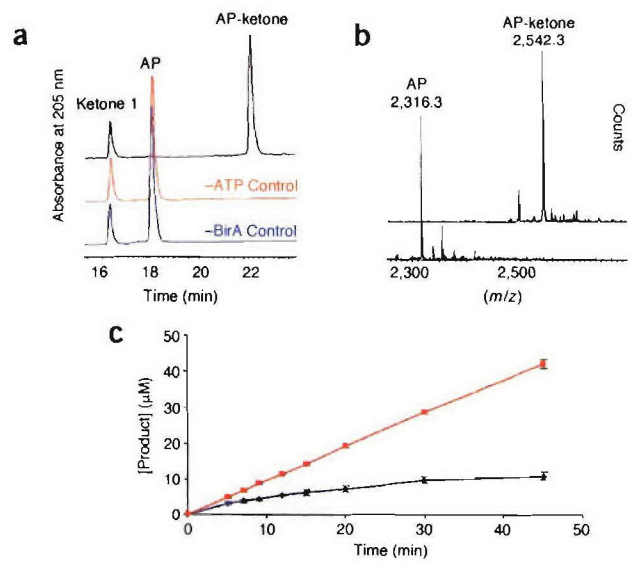

Figure 2 | BirA-catalyzed ligation of ketone 1 to the AP. (**a**) HPLC traces showing BirA- and ATP-dependent ligation of ketone 1 to a synthetic acceptor peptide (KKKGPGGLNDIFEAQKIEWH; acceptor lysine is underlined). (**b**) MALDI-TOF spectrum showing mass of purified AP-ketone conjugate. (**c**) Time course of biotin (■) and ketone 1 (◆) ligation to synthetic AP using 0.091 μM BirA. Each data point represents the average of three experiments. Error bars, 1 s.d.

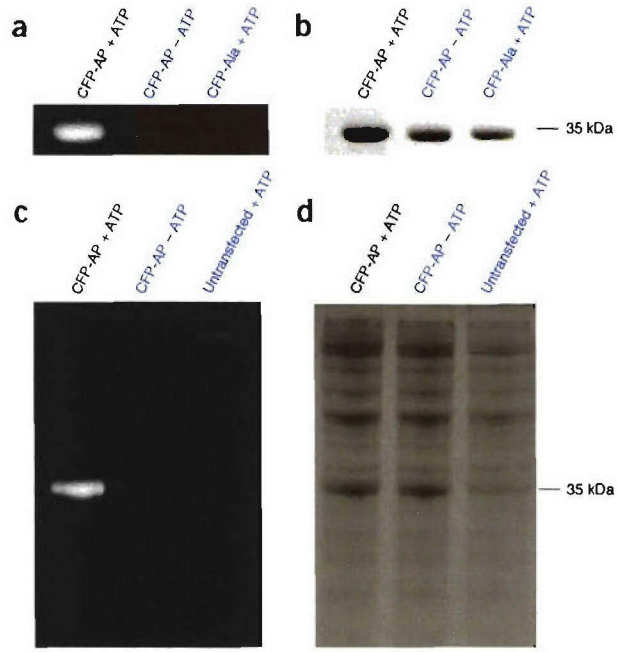

Figure 3 | Labeling of recombinant CFP-AP with fluorescein hydrazide. (**a**) Fluorescence gel image of denatured CFP-AP protein samples (fused AP sequence: GLNDIFEAQKIEWHE; acceptor lysine underlined) labeled by ketone 1 and fluorescein hydrazide. Omission of ATP (second lane) eliminates labeling, as does mutation of the acceptor lysine (CFP-Ala; third lane). (**b**) Coomassie blue–stained image of the gel in **a**. (**c**) Fluorescence image of CFP-AP–transfected HEK cell lysates labeled with ketone 1 and then with fluorescein hydrazide. Only the CFP-AP is labeled. Omission of ATP (second lane) eliminates labeling, and labeling is not seen when lysates are not transfected with the CFP-AP plasmid. (**d**) Coomassie blue–stained image of the gel in **c**.

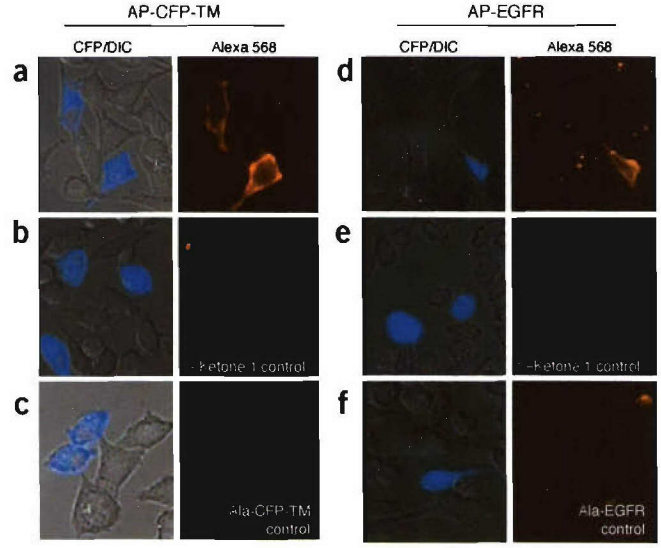

Figure 4 | Site-specific labeling of proteins expressed on the surface of live HeLa cells with BP. Cells expressing either the AP-CFP-TM construct (**a**–**c**) or AP-tagged EGFR (**d**–**f**) were labeled with ketone 1 for 60 min and then by BP for 60 min. The probe was then detected via its biotin handle using streptavidin-Alexa 568. The left columns show the CFP images (false-colored cyan) merged with the DIC images. The right columns show the Alexa 568 images (false-colored orange). (**a**) HeLa cells transfected with AP-CFP-TM are labeled with ketone 1 and BP, whereas untransfected neighboring cells are not. (**b**) Negative control without ketone 1. (**c**) Negative control with AP-CFP-TM replaced by the Ala-CFP-TM point mutant. (**d**) HeLa cells cotransfected with AP-EGFR and a cytoplasmic CFP marker plasmid show BP labeling, whereas untransfected neighboring cells are not labeled. (**e**) Negative control without ketone 1. (**f**) Negative control with AP-EGFR replaced by the Ala-EGFR point mutant.

transfected HEK cells was either treated with ketone 1 followed by fluorescein hydrazide, as above, or probed with anti-pentahistidine mouse antibody followed by fluorescein-conjugated secondary antibody (the CFP-AP construct bears an N-terminal hexahistidine tag). The fluorescence image of the resulting blot shows that our method is considerably more sensitive than antibody labeling for detection of CFP-AP in lysate (**Supplementary Fig. 1** online).

Labeling of cell surface proteins

Because ketones are absent from native cell surfaces, ketone 1 should permit the site-specific introduction of hydrazide or hydroxylamine probes onto AP-tagged cell surface proteins. To demonstrate this, we fused the AP to the N terminus of CFP and then attached this construct to the transmembrane (TM) domain of the platelet-derived growth factor receptor. The TM domain targets the entire construct to the cell surface, whereas CFP allows identification of transfected cells. This construct, called AP-CFP-TM, was efficiently expressed in HeLa cells 12–24 h after transfection. Direct enzymatic biotinylation with extracellular BirA confirmed that the AP tag was expressed on the cell surface and sterically accessible to BirA (data not shown). To highlight the scope of our methodology, we labeled AP-CFP-TM with a custom probe (benzophenone-biotin hydrazide, BP; structure shown in **Fig. 1c** and synthesis described in **Supplementary Methods** online), which bears a hydrazide for conjugation to ketone 1, a photocrosslinking-competent benzophenone moiety, and a biotin moiety to allow sensitive detection by streptavidin staining (separate experiments have shown that streptavidin does not bind to ketone 1 itself; data not shown).

To initiate labeling, the media was replaced with Dulbecco's phosphate buffered saline (DPBS), pH 7.4, containing BirA, ketone 1 and ATP. Because we were concerned about the possible toxicity of extracellular ATP, we separately examined the growth rate of HeLa cells incubated for 24 h with various amounts of ATP and observed no effect at concentrations below 5 mM; we therefore used 1 mM ATP for all our cellular experiments. The ketone ligation was allowed to proceed for 10–60 min. The cells were then rinsed to remove excess ketone, and BP was added in slightly acidic medium (DPBS, pH 6.2), which is known to accelerate hydrazone formation[16]. After cells were incubated for 10–60 min, streptavidin conjugated to the fluorophore Alexa 568 was used to detect the biotin handle of the BP probe. The fluorescence and differential interference contrast (DIC) images of the labeled cells are shown (**Fig. 4**). Cells transfected with AP-CFP-TM show distinct membrane labeling by the BP probe (as indicated by the streptavidin–Alexa 568 staining pattern), whereas neighboring untransfected cells remain unlabeled (**Fig. 4a**). Negative controls without ketone 1 (**Fig. 4b**) or with Ala-CFP-TM replacing AP-CFP-TM (**Fig. 4c**) show only background levels of staining, demonstrating that BP labeling proceeds via ketone 1 and is highly specific for the lysine of the AP tag. Despite the necessity of a two-stage labeling protocol, high levels of labeling

were achieved in as little as 20 min, which should allow our method to be used for the study of relatively fast biological processes, such as receptor trafficking.

We also used the AP-CFP-TM construct to quantify the sensitivity of BirA-catalyzed labeling. On a dish of cells expressing AP-CFP-TM at a range of concentrations (<10 μM to >1 mM as determined by comparison of fluorescence intensity to that of a wedge of purified CFP protein of known concentration; see **Supplementary Methods** online for details), labeling by the BP probe was clearly detectable, with a signal-to-background ratio >4:1, for cells expressing 10 μM or more of AP-CFP-TM. Based on deconvolution imaging, which shows approximately a 1:1 ratio of cell surface to intracellular AP-CFP-TM fluorescence (data not shown), and assuming an average cell volume of 1 pl, 10 μM expression level corresponds to $\sim 10^6$ copies of AP on the cell surface. Thus, our labeling method can detect cell surface proteins expressed at 10^6 copies per cell and perhaps even less.

To demonstrate BirA-mediated labeling of a natural protein, we selected the epidermal growth factor receptor (EGFR). The trafficking behavior and ligand-dependent dimerization, and possible higher-order oligomerization[17], of EGFR are of great biological interest. In addition, EGFR has proven intractable to study by extracellular GFP fusion, which severely impairs receptor expression and trafficking[18]. Thus, only minimal-sized probes and tags may be tolerated by the extracellular domain. We fused the AP to the N terminus of human EGFR, expressed the construct in HeLa cells and demonstrated both robust surface expression and steric accessibility of the AP tag using direct enzymatic biotinylation. We then used BirA- and ketone 1–mediated labeling to introduce the BP probe onto AP-EGFR. Cells cotransfected with AP-EGFR and cytoplasmic CFP (used as a transfection marker) show surface staining, whereas untransfected cells do not (**Fig. 4d**). Negative controls without ketone 1 (**Fig. 4e**) or with AP-EGFR replaced by Ala-EGFR (**Fig. 4f**) gave no labeling.

Because of its small size in comparison to the GFP tag, the 15-amino acid AP tag is less likely to alter the expression, trafficking or function of EGFR. We compared the distribution of AP-EGFR and untagged wild-type EGFR by immunofluorescence staining with anti-EGFR antibody and found no substantial difference (**Supplementary Fig. 2** online). In addition, EGF treatment elevates phosphotyrosine levels at the plasma membrane indistinguishably in wild-type EGFR- and AP-EGFR-transfected cells (**Supplementary Fig. 2** online), suggesting that the AP tag does not appreciably affect receptor function[19]. The AP tag at the N terminus thus seems to be minimally invasive and should allow the introduction of a range of probes with which to study EGFR trafficking and function in live cells.

DISCUSSION

We have developed new methodology for tagging cell surface proteins with biophysical probes using a 15-amino-acid AP sequence and the enzyme BirA. The method is highly specific because it capitalizes on the excellent sequence specificity of BirA, and it is versatile because the ketone platform allows the introduction of a wide range of probes. In these respects, BirA-based labeling compares favorably to existing labeling approaches, such as AGT[1], DHFR[2], FKBP[3] and ACP/PCP[4,5], which use large and hence more sterically invasive tags; and FlAsH[6], peptide aptamers[7] and Ni-NTA[8], which are less specific or rely on noncovalent interactions. Our method has disadvantages, however, and must therefore be seen as a complement to, rather than a replacement for, existing methodologies. The labeling is restricted to cell surface proteins because competing ketone- and aldehyde-containing small molecules inside cells most likely would prevent specific ligation of hydrazide- or hydroxylamine-functionalized probes to the target protein. It may be possible to surmount this problem through extensive washouts, as has been suggested[20], but our preferred approach will be to re-engineer BirA to accept other, more chemically orthogonal biotin analogs. We and others[11] have already shown that BirA can be expressed inside mammalian cells and retains its activity and specificity. Another limitation of our approach is the two-step labeling protocol, which limits the biological processes that can be studied based on their timescale. We report a minimal labeling time of 20 min, which is faster than that for techniques such as FlAsH, but slower than for AGT or ACP/PCP tagging strategies. Efforts are underway to accelerate the hydrazone formation reaction, in parallel with efforts to identify BirA mutants that accept probes of interest directly, providing a single-step labeling protocol.

Our method and the recently described ACP/PCP strategies represent, to our knowledge, the only reported examples of *in vivo* enzyme-mediated site-specific protein labeling (although *in vitro* labeling has been achieved using transglutaminase[21,22] and sortase[23] enzymes). A unique advantage of these methods is that labeling can be spatially controlled through genetic targeting of the labeling enzyme. For example, we are now working to target BirA to the presynaptic surface, to specifically label proteins at the postsynaptic surface of neurons. No other labeling methodology yet allows this degree of spatial control.

In conclusion, we have developed new protein labeling methodology that combines the specificity of GFP tagging with the minimal invasiveness of a small peptide. We demonstrated the labeling on a synthetic peptide, on purified protein, on mammalian cell lysate and on both an artificial construct and EGFR expressed on the surface of living mammalian cells. Both fluorophore and benzophenone attachment to EGFR should permit noninvasive study of receptor trafficking and oligomerization in live cells. Future efforts will focus on extending the methodology to intracellular labeling and improving the timescale of labeling, as well as on exploiting the enzyme dependence to spatially restrict labeling to interesting protein subpopulations.

METHODS

HPLC assay for probe ligation to synthetic AP. The synthetic AP with sequence KKKGPGGLNDIFEAQKIEWH was synthesized by the Tufts University Core Facility. The crude peptide was purified by reverse-phase HPLC (Microsorb-MV 300 C18 column, Varian; 10–39% acetonitrile in water with 0.1% TFA over 35 min, flow rate 4.7 ml/min); the desired peak had a retention time of 25.5 min. After lyophilization, the peptide was redissolved in water and the concentration was determined from the absorbance at 280 nm using the calculated extinction coefficient of 5690 $M^{-1}cm^{-1}$. Reaction conditions for the probe ligation to the AP were as follows: 50 mM bicine, pH 8.3, 5 mM magnesium acetate, 4 mM ATP, 100 μM AP, 1–2 μM BirA and 1 mM probe (either biotin or racemic ketone 1). Reactions were incubated at 30 °C for 1–2 h, then quenched through addition of 45 mM EDTA. Reactions were analyzed on a reverse-phase HPLC column

(Microsorb-MV 300 C18). Biotin ligation reactions were analyzed using a gradient of 10–43% acetonitrile in water with 0.1% TFA over 20 min (flow rate 1.0 ml/min); retention times were 8.2 min for biotin, 16.3 min for the AP and 17.7 min for the AP-biotin conjugate. Ketone 1 ligation reactions were analyzed using a gradient of 10–46% acetonitrile in water with 0.1% TFA over 25 min (flow rate 1.0 ml/min); retention times were 16.4 min for ketone 1, 17.9 min for the AP and 22.0 min for the AP–ketone 1 conjugate. For MALDI-TOF analysis, the product peak was collected, diluted with matrix solution (saturated α-cyano 4-hydroxycinnamic acid in 50% acetonitrile in water with 0.05% TFA) and spotted onto the sample target. Positive-ion MALDI-TOF data were acquired in reflector mode with external calibration.

Measurement of probe ligation kinetics. For kinetic measurements, the reaction conditions were the same as above except that 0.091 μM BirA was used, and for the ketone ligation reactions, 2 mM of racemic ketone 1 was used. A 400 μl reaction was initiated by addition of BirA and incubated at 30 °C. At various time points, a 40 μl aliquot was removed and quenched with EDTA. Reactions were analyzed by reverse-phase HPLC as described above. The area ratios of AP and AP-probe conjugate peaks were converted to concentrations of AP-probe conjugate using a calibration curve generated by mixing known ratios of AP and AP-probe conjugate. The concentration of AP-probe conjugate was plotted against time, and the reported initial rate was the slope of the line fit to the linear region of product synthesis.

Fluorescent labeling of CFP-AP. The reaction conditions for enzymatic ligation of ketone 1 to CFP-AP were as follows: 50 mM bicine, pH 8.3, 5 mM magnesium acetate, 4 mM ATP, 10–20 μM CFP-AP, 1.3 μM BirA and 100 μM racemic ketone 1. The reaction was incubated at 30 °C for 3 h, then 0.1 M HCl was added to adjust the pH to 6.2. Fluorescein hydrazide (Molecular Probes) was added to a final concentration of 1 mM, and the reaction was incubated at 30 °C for 12–16 h. Sodium cyanoborohydride (15 mM) was added to reduce the hydrazone for 1.5 h at 4 °C. The total protein was precipitated by addition of trichloroacetic acid (TCA) to a final vol/vol ratio of 10%. The protein pellet was redissolved in SDS-PAGE loading buffer, resolved by SDS-PAGE and visualized with the STORM 860 instrument (Amersham Biosciences).

Fluorescent labeling of CFP-AP in mammalian cell lysates. Human embryonic kidney 293T (HEK) cells were transfected with a pcDNA3 plasmid containing the CFP-AP gene (with an N-terminal hexahistidine tag) using Lipofectamine 2000 (Invitrogen) according to the manufacturer's instructions. Lysates were generated after 24–48 h at 70–80% confluence using a hypotonic lysis protocol to minimize protease release. Briefly, cells were concentrated by centrifugation and then resuspended in 1 mM HEPES, pH 7.5, 5 mM $MgCl_2$, 1 mM PMSF, 1 mM EGTA and protease inhibitor cocktail (Calbiochem). After incubation at 4 °C for 10 min, the cells were lysed by vigorous vortexing for 2 min at room temperature. The crude lysate was clarified by centrifugation, then divided into aliquots and stored at −80 °C. The reaction conditions for enzymatic ligation of ketone 1 were as follows: 50 mM bicine, pH 8.3, 5 mM magnesium acetate, 4 mM ATP, 1 μM BirA, 200 μM racemic ketone 1 and lysate to a final vol/vol ratio of 82%. The reactions were incubated at 30 °C for 4 h, then 0.1 M HCl was added to adjust the pH to 6.2. Fluorescein hydrazide was added to a final concentration of 1 mM, and the reaction was incubated at 30 °C for 20 h. After reduction with sodium cyanoborohydride (15 mM), the total protein was precipitated by addition of trichloroacetic acid to a final vol/vol ratio of 10%. The protein pellet was redissolved in SDS-PAGE loading buffer, resolved by SDS-PAGE and visualized with the STORM 860 instrument.

Labeling of cell surface AP-CFP-TM and AP-EGFR expressed in HeLa cells. HeLa cells were transfected with the AP-CFP-TM or AP-EGFR plasmid using Lipofectamine 2000 according to the manufacturer's instructions. After 12–24 h at 37 °C, the cells were washed twice with DPBS, pH 7.4. Enzymatic ligation of ketone 1 to AP-CFP-TM was performed in DPBS, pH 7.4, with 5 mM $MgCl_2$, 0.2 μM BirA, 1 mM racemic ketone 1 and 1 mM ATP for 10–60 min at 32 °C. Cells were then washed twice with DPBS, pH 6.2, and incubated for 10–60 min at 16 °C (to reduce endocytosis) with 1 mM BP in DPBS, pH 6.2. The cells were washed twice with DPBS, pH 7.4 and incubated with streptavidin-Alexa 568 (3 μg/ml; Molecular Probes) in DPBS, pH 7.4, and 1% BSA for 10 min at 4 °C. The cells were washed twice with DPBS, pH 7.4, and imaged in the same buffer on a Zeiss Axiovert 200M inverted epifluorescence microscope using a 40× oil-immersion lens. CFP (420DF20 excitation, 450DRLP dichroic, 475DF40 emission), Alexa 568 (560DF20 excitation, 585DRLP dichroic, 605DF30 emission) and DIC images (630DF10 emission) were collected and analyzed using OpenLab software (Improvision). Fluorescence images were background-corrected. Acquisition times ranged from 0.2–2 s.

Note: Supplementary information is available on the Nature Methods website.

ACKNOWLEDGMENTS

Funding was provided by the US National Institutes of Health (K22-HG002671-01), EJLB Foundation and Massachusetts Institute of Technology. I.C. was supported by a National Science Foundation predoctoral fellowship and a Wyeth Pharmaceuticals fellowship, and M.H. was supported by an MIT-Merck postdoctoral fellowship. We thank Tanabe USA for biotin, D. Beckett for the BirA plasmid and helpful advice, K.D. Wittrup for the EGFR plasmid, J.M. Baskin, E. McNeill and K.H. Riesenburger for assistance, and J.E. Wilson and G.C. Fu for use of their chiral HPLC. We also thank S.S. Licht and R.Y. Tsien for helpful advice.

COMPETING INTERESTS STATEMENT

The authors declare competing financial interests (see the *Nature Methods* website for details).

Received 19 July; accepted 20 December 2004
Published online at http://www.nature.com/naturemethods/

1. Keppler, A., Pick, H., Arrivoli, C., Vogel, H. & Johnsson, K. Labeling of fusion proteins with synthetic fluorophores in live cells. *Proc. Natl. Acad. Sci. USA* **101**, 9955–9959 (2004).
2. Miller, L.W., Sable, J., Goelet, P., Sheetz, M.P. & Cornish, V.W. Methotrexate conjugates: a molecular *in vivo* protein tag. *Angew. Chem. Int. Edn. Engl.* **43**, 1672–1675 (2004).
3. Marks, K.M., Braun, P.D. & Nolan, G.P. A general approach for chemical labeling and rapid, spatially controlled protein inactivation. *Proc. Natl. Acad. Sci. USA* **101**, 9982–9987 (2004).
4. George, N., Pick, H., Vogel, H., Johnsson, N. & Johnsson, K. Specific labeling of cell surface proteins with chemically diverse compounds. *J. Am. Chem. Soc.* **126**, 8896–8897 (2004).
5. Yin, J., Liu, F., Li, X. & Walsh, C.T. Labeling proteins with small molecules by site-specific posttranslational modification. *J. Am. Chem. Soc.* **126**, 7754–7755 (2004).

6. Adams, S.R. *et al.* New biarsenical ligands and tetracysteine motifs for protein labeling *in vitro* and *in vivo*: Synthesis and biological applications. *J. Am. Chem. Soc.* **124**, 6063–6076 (2002).
7. Marks, K.M., Rosinov, M. & Nolan, G.P. *In vivo* targeting of organic calcium sensors via genetically selected peptides. *Chem. Biol.* **11**, 347–356 (2004).
8. Guignet, E.G., Hovius, R. & Vogel, H. Reversible site-selective labeling of membrane proteins in live cells. *Nat. Biotechnol.* **22**, 440–444 (2004).
9. Chen, I. & Ting, A.Y. Site-specific labeling of proteins with small molecules in live cells. *Curr. Opin. Biotech.* (in the press).
10. Beckett, D., Kovaleva, E. & Schatz, P.J. A minimal peptide substrate in biotin holoenzyme synthetase-catalyzed biotinylation. *Protein Sci.* **8**, 921–929 (1999).
11. de Boer, E. *et al.* Efficient biotinylation and single-step purification of tagged transcription factors in mammalian cells and transgenic mice. *Proc. Natl. Acad. Sci. USA* **100**, 7480–7485 (2003).
12. Mahal, L.K., Yarema, K.J. & Bertozzi, C.R. Engineering chemical reactivity on cell surfaces through oligosaccharide biosynthesis. *Science* **276**, 1125–1128 (1997).
13. Baraldi, P.G. *et al.* Synthesis of sulfur-containing carbaprostacyclin analogs. *Gazz. Chim. Ital.* **114**, 177–183 (1984).
14. Lavielle, S., Bory, S., Moreau, B., Luche, M.J. & Marquet, A. Total synthesis of biotin based on stereoselective alkylation of sulfoxides. *J. Am. Chem. Soc.* **100**, 1558–1563 (1978).
15. Chapman-Smith, A., Morris, T.W., Wallace, J.C. & Cronan, J.E., Jr. Molecular recognition in a post-translational modification of exceptional specificity. Mutants of the biotinylated domain of acetyl-CoA carboxylase defective in recognition by biotin protein ligase. *J. Biol. Chem.* **274**, 1449–1457 (1999).
16. Nauman, D.A. & Bertozzi, C.R. Kinetic parameters for small-molecule drug delivery by covalent cell surface targeting. *Biochim. Biophys. Acta* **1568**, 147–154 (2001).
17. Lax, I. *et al.* Epidermal growth factor (EGF) induces oligomerization of soluble, extracellular, ligand-binding domain of EGF receptor. A low resolution projection structure of the ligand-binding domain. *J. Biol. Chem.* **266**, 13828–13833 (1991).
18. Brock, R., Hamelers, I.H. & Jovin, T.M. Comparison of fixation protocols for adherent cultured cells applied to a GFP fusion protein of the epidermal growth factor receptor. *Cytometry* **35**, 353–362 (1999).
19. Reynolds, A.R., Tischer, C., Verveer, P.J., Rocks, O. & Bastiaens, P.I. EGFR activation coupled to inhibition of tyrosine phosphatases causes lateral signal propagation. *Nat. Cell Biol.* **5**, 447–453 (2003).
20. Zhang, Z. *et al.* A new strategy for the site-specific modification of proteins in vivo. *Biochemistry* **42**, 6735–6746 (2003).
21. Huff, T. *et al.* Thymosin β(4) serves as a glutaminyl substrate of transglutaminase. Labeling with fluorescent dansylcadaverine does not abolish interaction with G-actin. *FEBS Lett* **464**, 14–20 (1999).
22. Dutton, A. & Singer, S.J. Crosslinking and labeling of membrane proteins by transglutaminase-catalyzed reactions. *Proc. Natl. Acad. Sci. USA* **72**, 2568–2571 (1975).
23. Mao, H., Hart, S.A., Schink, A. & Pollok, B.A. Sortase-mediated protein ligation: a new method for protein engineering. *J. Am. Chem. Soc.* **126**, 2670–2671 (2004).

Phosphorylation Reporters

A Genetically Encoded Fluorescent Reporter of Histone Phosphorylation in Living Cells**

*Chi-Wang Lin and Alice Y. Ting**

Histones, the scaffolding proteins around which DNA is wrapped in chromatin, participate in transcriptional regulation by controlling steric access to DNA and providing docking sites for nuclear proteins. One of the major mechanisms for this regulation is post-translational modification; phosphorylation, acetylation, and methylation of the N-terminal tails of histone proteins, especially histones H3 and H4, alter the shape, charge, and hydrophobicity of the nucleosome core particle, affecting its interactions with transcription factors, polymerases, and other chromatin-associated proteins.[1] Since post-translational modifications of histones represent one of the earliest control points for the regulation of gene transcription, it is important to develop sensitive and accurate methods for detecting them, ideally within intact, living mammalian cells. Existing methods, such as chromatin immunoprecipitation and immunofluorescence staining, require cell lysis or membrane permeabilization and therefore sacrifice spatial and/or temporal information. Here we report the development of a fluorescent reporter that can detect phosphorylation of histone H3 at serine 28 in intact, single cells in real time.

The reporter design is shown in Figure 1a. A peptide substrate corresponding to the 30 N-terminal amino acids of histone H3 is joined to a phosphoserine/threonine-binding module by a flexible linker, and this fusion protein is sandwiched between a pair of green-fluorescent protein (GFP) mutants capable of fluorescence resonance energy transfer (FRET): cyan-fluorescent protein (CFP) and yellow-fluorescent protein (YFP).[2–4] On enzymatic phosphorylation of the histone H3 peptide, the phosphoserine/threonine-binding domain should form an intramolecular complex with the phosphopeptide, altering the spatial relationship between the flanking CFP and YFP units and changing the FRET level. Dephosphorylation of the substrate peptide by a phosphatase should cause the intramolecular complex to dissociate, restoring the original FRET level. We previously used this general design to develop phosphorylation reporters for consensus substrates of the epidermal growth factor

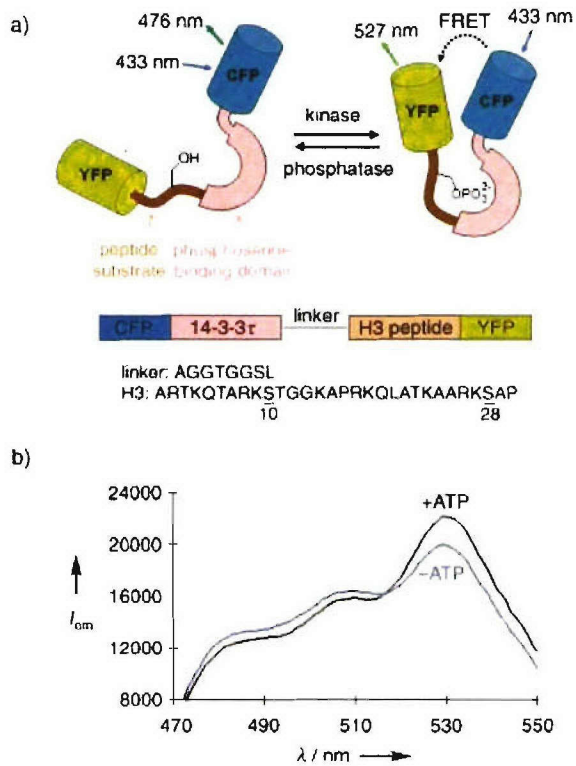

Figure 1. a) Reporter design and domain structure. The two serine-phosphorylation sites in the H3 peptide are underlined. b) Normalized reporter emission spectra before (blue) and after (black) phosphorylation by Msk-1 kinase (excitation at 433 nm).

[*] C.-W. Lin, Prof. A. Y. Ting
Department of Chemistry, Room 18-496
Massachusetts Institute of Technology
Cambridge, MA 02139 (USA)
Fax: (+1) 617-258-8150
E-mail: ating@mit.edu

[**] This work was supported by MIT start-up funds and by grants from the National Institutes of Health (K22-HG002671-01), the Office of Naval Research (N00014-03-1-0456), and the Camille and Henry Dreyfus New Faculty Award Program (NF-02-003). C.-W.L. was supported by a Merck/MIT predoctoral fellowship. The Multiuser Facility for the Study of Complex Macromolecular Systems (NSF-0070319) is also gratefully acknowledged. The Msk-1 expression plasmid was a gift from Prof. Jiahuai Han. We are grateful to Sean Liu and Dr. Brian J. Schneider for technical assistance, and to Profs. Jin Zhang and Michael B. Yaffe for helpful discussions.

Supporting information for this article is available on the WWW under http://www.angewandte.org or from the author.

  DOI: 10.1002/anie.200353375

receptor (EGFR), Src kinase, and Abl kinase,[3] while others have used this approach to develop reporters for protein kinase A,[4] protein kinase C,[5] and the insulin receptor.[6] The phosphoserine/threonine-binding module in the reporter described herein, which represents the first for histones, is the signaling protein 14-3-3τ,[7] which consists of 232 amino acids and naturally binds to the phosphorylated form of residues 615–644 of Cbl,[8] a sequence similar to residues 1–30 of H3.

We constructed the reporter gene by standard cloning methods (GenBank accession no. AY422821), expressed the His_6-tagged recombinant protein in *E. coli*, and purified it by nickel affinity chromatography. In in vitro assays with purified Msk-1 kinase, which phosphorylates both serine 10 and 28 of H3,[9] the reporter gave a 25% increase in the YFP/CFP emission ratio (Figures 1b and 2a). Leaving out either ATP or

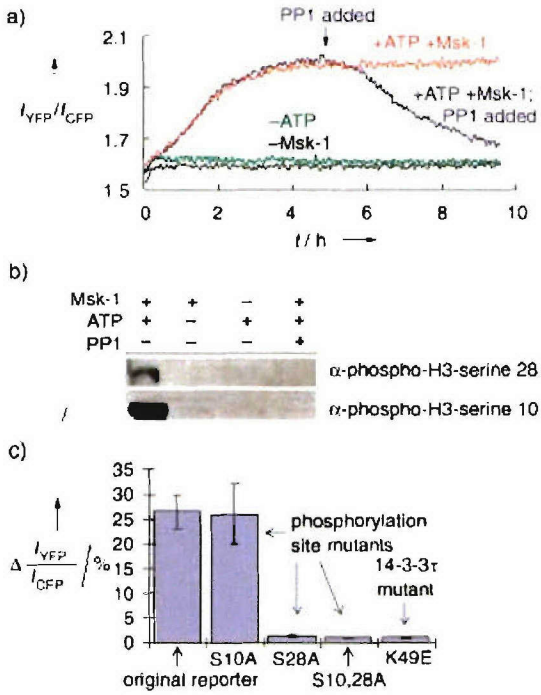

Figure 2. a) Change in the reporter YFP/CFP emission ratio over time under various reaction conditions. b) Immunoblot analysis of the four reactions in (a) after 10 h with anti-phospho-H3-serine 10 and -serine 28 antibodies. c) Maximal emission ratio changes observed in phosphorylation reactions with four reporter mutants. Each measurement was performed in triplicate.

the enzyme abolished the FRET change (Figure 2a). To examine reporter reversibility, we treated the phosphorylated reporter protein with PP1, a broad-specificity serine/threonine phosphatase.[10] Over about 5 h, the FRET returned to its original level (Figure 2a). Reporter protein from each reaction in Figure 2a was also analyzed by an anti-phospho-H3-serine 10 and -serine 28 immunoblot. Figure 2b shows a good correspondence between the FRET level and this traditional method for determining the phosphorylation state of a protein. Lastly, the phosphorylation rate of the in vitro reporter is very similar to that of full-length H3 under identical conditions (data not shown), which indicates that the former is a good mimic of the latter.

Because the N-terminus of H3 contains two potential phosphorylation sites (serine 10 and serine 28), we performed site-directed mutagenesis on the reporter to determine which site(s) were responsible for the FRET increase. Figure 2c shows that mutation of serine 10 to a phosphorylation-incompetent alanine had no effect on the reporter response, whereas mutation of serine 28 to alanine abolished the FRET change. These results indicate that the reporter specifically responds to serine 28 phosphorylation. Because we wondered whether this specificity was a consequence of the reporter geometry or reflected an inherent selectivity of the 14-3-3τ domain for phosphoserine 28, we constructed another reporter identical to the original but with the 14-3-3τ and histone peptide domains transposed. Interestingly, this reporter was responsive to phosphorylation at both the serine 10 and serine 28 positions (see Supporting Information), which suggests that geometrical constraints determine the specificity of the original reporter.

A charge-reversal mutation in the binding pocket of the 14-3-3τ domain (K49E), expected to abolish the binding affinity of the 14-3-3τ domain for phosphoserine,[7] also eliminated the FRET response (Figure 2c). This is consistent with the designed mechanism for sensing of phosphorylation through FRET. We wondered, however, whether the known dimerization potential of 14-3-3τ,[7] also demonstrated in a previous 14-3-3τ-based reporter,[4] would lead to dimerization of our reporter. Analytical ultracentrifugation confirmed that our reporter exists as a dimer in solution (data not shown). Therefore, the fluorescence response of our reporter might be due either to true intramolecular binding or to intermolecular binding across the dimer interface.

To test the histone phosphorylation reporter in living cells, we appended a nuclear localization sequence (PKKKRK) to the C-terminus of the reporter gene and introduced the plasmid DNA into HeLa cells by lipofection. The reporter was efficiently expressed after about 12 h. Because previous studies have shown that serine 28 phosphorylation levels transiently increase during the mitotic (M) phase of the cell cycle,[11] we monitored the FRET level of our reporter in dividing HeLa cells over 26 h. As shown in Figure 3 and in the movie provided as Supporting Information, the reporter displayed a rapid increase in YFP/CFP emission ratio (15–25%) that, in eight separate cells, closely preceded breakdown of the nuclear envelope (as measured by reporter distribution in the cell) by 5–15 min. The high FRET was sustained for several hours and then dropped slowly after cytokinesis, or separation of the cytoplasm into daughter cells. A control experiment with the S28A mutant of the reporter did not give a FRET change during cell division, demonstrating that the response of the reporter is not an artifact of changes in reporter concentration or cellular pH over the course of cell division (see Figure 3b).

Elevated serine 10 and 28 phosphorylation levels have both been linked to mitosis,[12,13] but the precise molecular roles of these modifications have yet to be elucidated. Our study provides a high-resolution picture of serine 28 phosphorylation onset and disappearance in single living HeLa

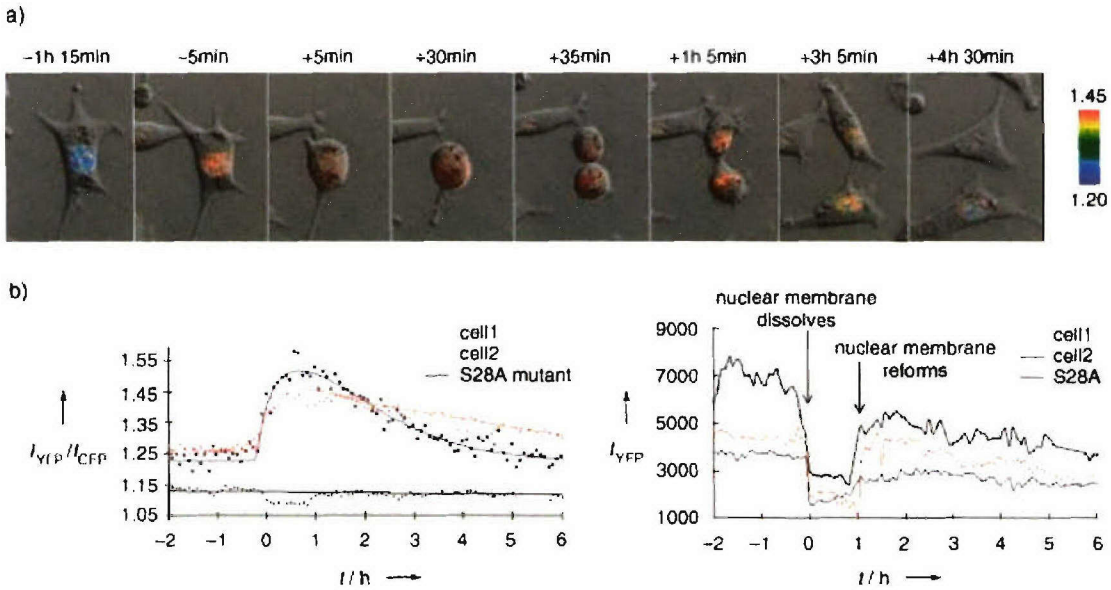

Figure 3. a) Reporter response during HeLa cell division. The bar on the right shows the correlation between YFP/CFP emission ratio and cell pseudocolor. The indicated times refer to hours/minutes after nuclear-membrane breakdown. b) Emission ratio and YFP emission intensity as a function of time after nuclear-membrane breakdown for two cells expressing the reporter and one cell expressing the S28A reporter mutant (t = time after nuclear-membrane breakdown).

cells during cell division. We find a previously unobserved correlation between serine 28 phosphorylation onset and nuclear-envelope breakdown, which may suggest a mechanism for coordinating changes in chromatin and cell morphology during the M phase. Future investigation will follow up on this intriguing possibility. In another avenue for future study, if the phosphorylation reporter were physically anchored to chromatin (for example, through genetic fusion to one of the four histone proteins), spatial resolution might be further increased.

The work described herein also demonstrates the capabilities and limitations of current methodology for the design of fluorescent reporters. Without a recognition element known a priori to bind the phosphorylated histone sequence, we developed a reporter for H3 serine 28. In fact, the 14-3-3τ domain consensus recognition sequence is quite different from the peptide sequence flanking serine 28.[14] Either 14-3-3τ binding is significantly more promiscuous and context-dependent than previously thought, or our reporter design can accommodate recognition domains of only modest intermolecular affinity for the substrate peptide. On the other hand, the impressive, geometry-sensitive specificity of our reporter for H3 serine 28 over other phosphorylation-competent sites in the same substrate peptide indicates a keen dependence on reporter design elements such as spacing and orientation of the binding domain and the substrate peptide.

In conclusion, this reporter, and similar ones such as histone methylation reporters[15] and acetylation reporters under development in our laboratory, should allow the study of transcriptional regulation in cells with greatly improved spatiotemporal resolution.

Experimental Section

The reporter gene was ligated into the pRSETB vector (Invitrogen, Carlsbad, CA) between the *Bam*HI and *Eco*RI sites, which installs a His_6 tag at the N-terminus. For protein expression, the plasmid was introduced into BL21(DE3) bacteria (Stratagene, La Jolla, CA) and the cells were grown in Luria Broth supplemented with ampicillin (100 μg mL^{-1}) at 37 °C until OD_{600} 0.5. Isopropyl-β-D-thiogalactopyranoside (IPTG) was then added to a final concentration of 0.4 mM to induce reporter expression. The cells were grown for 3 h at 30 °C and then harvested by centrifugation. Cells were lysed by sonication at 4 °C (six 30-second pulses at half-maximal power with 1 min between each pulse) in lysis buffer (50 mM Tris pH 7.8, 300 mM NaCl, 4 mM PMSF, and ¼ EDTA-free protease inhibitor cocktail tablet (Roche, Indianapolis, IN) per 10 mL of lysis buffer). The His_6-tagged reporter was purified from the lysate using a Ni-NTA agarose column (Qiagen, Valencia, CA) following the manufacturer's protocol. Fractions containing the reporter were pooled and transferred into TBS (140 mM NaCl, 3 mM KCl, 25 mM Tris pH 7.4) by two rounds of dialysis for storage in aliquots at −80 °C. Typical yields were 100–500 μg of protein per 0.5 L culture. Msk-1 kinase was prepared in an identical manner using the Msk-1-expression plasmid (His_6-tagged human Msk-1 in pET-11 vector (Novagen, Madison, WI)) that we received from Prof. Dr. Jiahuai Han.

Reaction conditions for the in vitro phosphorylation assays were as follows: 1–5 μM reporter, 0.6 mM ATP, 20 mM Hepes pH 7.7, 10 mM $MgCl_2$, 0.1 mM EGTA, 0.5 mM DTT, and 4 μM of Msk-1. Reactions were incubated at 30 °C for the indicated times. The phosphorylation state of the reporter from the in vitro assays was analyzed by Western blot using 12% SDS-PAGE gel, anti-phospho-H3-serine 10 antibody (Cell Signaling Technology, Beverly, MA) or anti-phospho-H3-serine 28 antibody (Upstate Biotechnology, Charlottesville, VA) (both at 1/1000 dilution for 3 h at 25 °C), and goat anti-rabbit-HRP conjugate or goat anti-mouse-HRP conjugate (1/1000 dilution for 2 h at 25 °C) (Bio-Rad, Hercules, CA). The HRP was visualized by chemiluminescence (Supersignal West Pico, Pierce, Rockford, IL).

pcDNA3 (Invitrogen, Carlsbad, CA) plasmid containing the reporter gene between the *Bam*HI and *Eco*RI sites was introduced

into HeLa cells by transfection with Fugene 6 (Roche, Indianapolis, IN). Images were collected 8–24 h after transfection on a Zeiss Axiovert 200M inverted epifluorescence microscope with differential interference contrast (DIC). Cells were maintained in 10% fetal bovine serum in phenol red-free DMEM (Invitrogen, Carlsbad, CA) at 37 °C under 5% CO_2 during imaging with an environmental control system (Solent Scientific, Portsmouth, UK) that housed the microscope stage. At each time point, four images were collected in rapid succession (automated, using OpenLab software (Improvision, Lexington, MA)): a CFP image (420DF20 excitation, 450DRLP dichroic, 475DF40 emission), a FRET image (420DF20 excitation, 450DRLP dichroic, 530DF30 emission), a YFP image (495DF10 excitation, 515DRLP dichroic, 530DF30 emission), and a DIC image (775DF50 emission). Fluorescence images were background corrected. Acquisition times ranged from 100 to 800 ms. The emission ratio image was generated by dividing the FRET image by the CFP image. The data shown in Figure 3a are a merge between the emission ratio image and the DIC image. The YFP intensity graph shown in Figure 3b was generated from the YFP images.

Received: November 21, 2003
Revised: March 19, 2004 [Z53375]

Keywords: fluorescence · histones · imaging · phosphorylation · reporters

[1] W. Fischle, Y. Wang, C. D. Allis, *Curr. Opin. Cell Biol.* **2003**, *15*, 172–183.
[2] J. Zhang, R. E. Campbell, A. Y. Ting, R. Y. Tsien, *Nat. Rev. Mol. Cell Biol.* **2002**, *3*, 906–918.
[3] A. Y. Ting, K. H. Kain, R. L. Klemke, R. Y. Tsien, *Proc. Natl. Acad. Sci. USA* **2001**, *98*, 15003–15008.
[4] J. Zhang, Y. Ma, S. S. Taylor, R. Y. Tsien, *Proc. Natl. Acad. Sci. USA* **2001**, *98*, 14997–15002.
[5] J. D. Violin, J. Zhang, R. Y. Tsien, A. C. Newton, *J. Cell Biol.* **2003**, *161*, 899–909.
[6] M. Sato, T. Ozawa, K. Inukai, T. Asano, Y. Umezawa, *Nat. Biotechnol.* **2002**, *20*, 287–294.
[7] H. Fu, R. R. Subramanian, S. C. Masters, *Annu. Rev. Pharmacol. Toxicol.* **2000**, *40*, 617–647.
[8] Y. C. Liu, Y. Liu, C. Elly, H. Yoshida, S. Lipkowitz, A. Altman, *J. Biol. Chem.* **1997**, *272*, 9979–9985.
[9] A. Soloaga, S. Thomson, G. R. Wiggin, N. Rampersaud, M. H. Dyson, C. A. Hazzalin, L. C. Mahadevan, J. S. Arthur, *EMBO J.* **2003**, *22*, 2788–2797.
[10] P. T. Cohen, *J. Cell Sci.* **2002**, *115*, 241–256.
[11] H. Goto, Y. Tomono, K. Ajiro, H. Kosako, M. Fujita, M. Sakurai, K. Okawa, A. Iwamatsu, T. Okigaki, T. Takahashi, M. Inagaki, *J. Biol. Chem.* **1999**, *274*, 25543–25549.
[12] Y. Wei, C. A. Mizzen, R. G. Cook, M. A. Gorovsky, C. D. Allis, *Proc. Natl. Acad. Sci. USA* **1998**, *95*, 7480–7484.
[13] M. J. Hendzel, Y. Wei, M. A. Mancini, A. Van Hooser, T. Ranalli, B. R. Brinkley, D. P. Bazett-Jones, C. D. Allis, *Chromosoma* **1997**, *106*, 348–360.
[14] M. B. Yaffe, A. E. Elia, *Curr. Opin. Cell Biol.* **2001**, *13*, 131–138.
[15] C. W. Lin, C. Y. Jao, A. Y. Ting, *J. Am. Chem. Soc.* **2004**, in press..

J|A|C|S
COMMUNICATIONS

Published on Web 04/23/2004

Genetically Encoded Fluorescent Reporters of Histone Methylation in Living Cells

Chi-Wang Lin, Cindy Y. Jao, and Alice Y. Ting*

Department of Chemistry, Massachusetts Institute of Technology, Cambridge, Massachusetts 02139

Received October 3, 2003; E-mail: ating@mit.edu

Post-translational protein modifications are used by cells to dynamically regulate protein structure and function. This regulation is particularly pronounced on histone proteins, the scaffolding proteins around which DNA is wrapped in chromatin. Phosphorylation, acetylation, and methylation of the N-terminal tails of histone proteins strongly influence transcription of neighboring genes by altering steric access to DNA and by introducing or removing protein docking sites.[1] Despite the importance of these modifications, few methods exist for detecting them, and none are effective in intact, living cells. Here, we describe a new class of fluorescent reporters that can be used in single, living cells to track histone methylation with high spatial and temporal resolution.

The general reporter design is shown in Figure 1a. A peptide substrate corresponding to the methylation site of interest within histone protein H2A, H2B, H3, or H4 is joined via a flexible linker to a methyllysine binding domain known as a chromodomain. Recently discovered, chromodomains are small (~55 amino acid), monomeric domains found in a variety of nuclear signaling proteins that bind with 1−200 μM K_d to lysine-methylated peptides but not to their unmethylated counterparts.[2] This fusion construct is sandwiched between a pair of fluorescence resonance energy transfer (FRET)-capable green fluorescent protein (GFP) mutants, cyan fluorescent protein (CFP) and yellow fluorescent protein (YFP). On enzymatic methylation of the histone-derived peptide, the chromodomain forms an intramolecular complex with the methyllysine side chain, altering the spatial relationship between the flanking CFP and YFP units, and changing the FRET level. Reversal of this FRET change would be evidence for a conjectured but so far undetected histone demethylase activity. This general design, in which a conformationally sensitive natural or engineered protein is sandwiched between two GFP mutants capable of FRET, has been successfully used to detect a range of intracellular molecules and biochemical events, including Ca^{2+}, cGMP, Ras activity, protease activity, and phosphorylation.[3] Our reporters are the first for detecting protein methylation.

We constructed methylation reporters for two lysine positions in histone H3 (K9 and K27) known to be involved in transcriptional repression,[4] X-inactivation,[5] and cellular differentation.[6] The genes for the two reporters (domain structures shown in Figure 1b) were assembled by standard cloning methods (GenBank accession nos. AY422822 and AY422823; see Supporting Information for details). The K9 reporter uses the HP1 chromodomain (residues 21−76) to recognize lysine 9 methylation in the context of residues 1−13 of histone H3,[7,8] while the K27 reporter uses the Polycomb (Pc) chromodomain (residues 21−78) to recognize lysine 27 methylation in the context of residues 24−35 of histone H3.[9,10] When H3 peptides spanning both lysines are incorporated, each chromodomain shows some crossover binding (Ting and Lin, unpublished observations); therefore, these shorter substrate sequences must be used. Crystallographic data[7−10] and peptide modification experiments[11] suggest that these shorter sequences are still specific

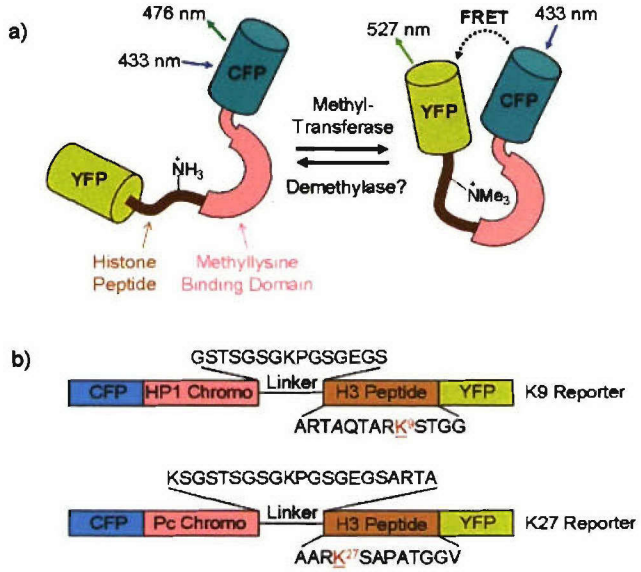

Figure 1. (a) General histone methylation reporter design. (b) Domain structures of two methylation reporters. The K9 reporter, top, uses the HP1 chromodomain for recognition of methylated K9 from the histone H3 N-terminus. An alternative methylation site at K4 in the original substrate has been mutated to alanine (italicized). The K27 reporter, bottom, uses the Polycomb (Pc) chromodomain for recognition of methylated K27 from histone H3.

substrates for histone methyltransferase enzymes and retain binding affinity for chromodomains. We estimated from cocrystal structures[7−10] that 15- and 21-residue linkers for the K9 and K27 reporters, respectively, would suffice to allow intramolecular complexation between the two linked domains.

Both reporters were overexpressed in *E. coli* and purified by nickel affinity chromatography. Reporter responsivity was assessed in vitro through measurement of the YFP/CFP emission ratio ($I_{527\ nm}/I_{476\ nm}$) in response to methylation by vSET, a histone H3 methyltransferase from *Paramecium bursaria* chlorella virus.[11] Figure 2a shows that both K9 and K27 reporters give emission ratio increases (60% and 28%, respectively) that depend on the presence of both enzyme and methyl donor, *S*-adenosyl methionine (SAM). To confirm a correlation between reporter FRET level and methylation state, and to examine the specificity of enzymatic methylation, we digested reporter protein from each reaction shown in Figure 2a with the protease Glu-C and analyzed the peptide fragments by MALDI-TOF (data in Supporting Information). The K9 reporter from the +vSET/+SAM reaction was cleanly trimethylated at lysine 9 after 10 h (no mono- or dimethylation detected), while the −SAM negative control contained only unmodified reporter protein. The K27 reporter was di- and trimethylated in the +vSET/+SAM reaction, while the corresponding negative controls contained only unmodified protein.

10.1021/ja038854h CCC: $27.50

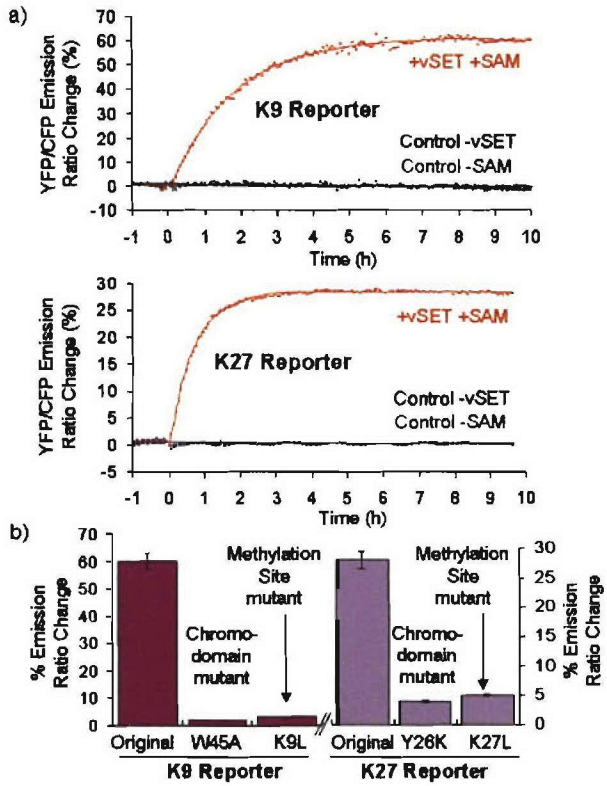

Figure 2. (a) Time-course graphs showing the emission ratio responses of the K9 and K27 reporters to enzymatic methylation by vSET (excitation at 433 nm). (b) Maximal emission ratio changes observed in vSET methylation reactions with various reporter mutants.

Site-directed mutagenesis was also used to examine the specificities and FRET response mechanisms of the two reporters (Figure 2b). Mutation of lysine 9 of the K9 reporter to a methylation-incompetent leucine (K9L) abolished the FRET response to vSET methylation. Similarly, mutation of lysine 27 of the K27 reporter (K27L) eliminated that reporter's response. The chromodomains of each reporter were also modified to eliminate affinity for methylated lysine (W45A[8] for the K9 reporter, and Y26K[10] for the K27 reporter). Both chromodomain mutants were unresponsive to enzymatic methylation, consistent with a FRET increase mechanism based on complexation between methyllysine side chain and chromodomain.

To test the K9 reporter in living cells, we appended a nuclear localization sequence (PKKKRK) to the C-terminal end of the reporter gene. The plasmid containing the reporter gene was then introduced by lipofection into both wild-type mouse embryonic fibroblasts (MEFs) and sister cells lacking the major K9-H3-specific methyltransferases Suv39h1 and Suv39h2 (Suv39h -/-).[12] Previous studies have shown that these cells exhibit drastically reduced levels of K9-H3 methylation in comparison to wild-type MEFs.[12] The reporter was efficiently expressed in both cell lines after 12 h. Measurement of YFP/CFP emission ratios showed that FRET levels were lower on average in Suv39h -/- cells than in wild-type MEFs (Figure 3; $n = 278$ cells, $\sigma = 0.163$, $p < 0.001$), demonstrating that our K9 construct can effectively report variations in methylation levels across different cell lines.

In conclusion, we have developed new fluorescent reporters of histone methylation that are effective in vitro and in single living

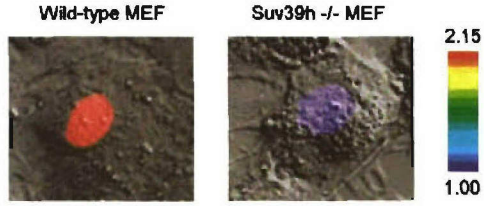

Figure 3. Basal YFP/CFP emission ratios of the K9 reporter expressed in wild-type mouse embryonic fibroblasts (MEFs) and sister cells lacking the K9-H3 methyltransferases Suv39h1 and Suv39h2. The bar on the right shows the correlation between YFP/CFP emission ratio and cell pseudocolor.

cells. By permitting investigators to record information nondestructively over time, our methodology should complement traditional techniques for detecting protein methylation, such as immunofluorescence or immunoprecipitation.[13] Although not demonstrated here, the spatial resolution could be greatly improved if the reporter were targeted through genetic fusion to specific intranuclear sites, such as transcription factor complexes or chromatin itself. Particularly in light of recent reports that histone methylation can be quite dynamic,[4,14] these reporters should find application in studies of gene silencing, X-inactivation, and cell differentiation, as well as in screening for the conjectured histone demethylase activity and for small-molecule inhibitors of methyltransferase activity.

Acknowledgment. We thank Sean Liu, Michael A. Gelman, Christine Yu, C. David Allis, and Yi Zhang for their advice and assistance. C.-W.L. and C.Y.J. were supported by the Merck/MIT fellowship and MIT's UROP program, respectively. The Polycomb, HP1, and vSET genes were gifts from Yi Zhang, Sepideh Khorasanizadeh, and Ming-Ming Zhou, respectively. The wild-type MEFs and Suv39h -/- sister cells were gifts from Thomas Jenuwein. We thank the NIH (K22-HG002671-01), ONR (N00014-03-1-0456), Dreyfus Foundation (NF-02-003), and MIT for funding.

Supporting Information Available: MALDI-TOF spectra of methylated K9 and K27 reporter proteins. Experimental protocols for cloning, reporter expression, methylation assays, and cell imaging. This material is available free of charge via the Internet at http://pubs.acs.org.

References

(1) Felsenfeld, G.; Groudine, M. *Nature* **2003**, *421*, 448−453.
(2) Jones, D. O.; Cowell, I. G.; Singh, P. B. *BioEssays* **2000**, *22*, 124−137.
(3) Zhang, J.; Campbell, R. E.; Ting, A. Y.; Tsien, R. Y. *Nat. Rev. Mol. Cell Biol.* **2002**, *3*, 906−918.
(4) Kim, J.; Jia, L.; Tilley, W. D.; Coetzee, G. A. *Nucleic Acids Res.* **2003**, *31*, 6741−6747.
(5) Plath, K.; Fang, J.; Mlynarczyk-Evans, S. K.; Cao, R.; Worringer, K. A.; Wang, H.; de la Cruz, C. C.; Otte, A. P.; Panning, B.; Zhang, Y. *Science* **2003**, *300*, 131−135.
(6) Ait-Si-Ali, S.; Guasconi, V.; Fritsch, L.; Yahi, H.; Sekhri, R.; Naguibneva, I.; Robin, P.; Cabon, F.; Polesskaya, A.; Harel-Bellan, A. *EMBO J.* **2004**, *23*, 605−615.
(7) Nielsen, P. R.; Nietlispach, D.; Mott, H. R.; Callaghan, J.; Bannister, A.; Kouzarides, T.; Murzin, A. G.; Murzina, N. V.; Laue, E. D. *Nature* **2002**, *416*, 103−107.
(8) Jacobs, S. A.; Khorasanizadeh, S. *Science* **2002**, *295*, 2080−2083.
(9) Min, J.; Zhang, Y.; Xu, R. M. *Genes Dev.* **2003**, *17*, 1823−1828.
(10) Fischle, W.; Wang, Y.; Jacobs, S. A.; Kim, Y.; Allis, C. D.; Khorasanizadeh, S. *Genes Dev.* **2003**, *17*, 1870−1881.
(11) Manzur, K. L.; Farooq, A.; Zeng, L.; Plotnikova, O.; Koch, A. W.; Sachchidanand; Zhou, M. M. *Nat. Struct. Biol.* **2003**, *10*, 187−196.
(12) Peters, A. H.; O'Carroll, D.; Scherthan, H.; Mechtler, K.; Sauer, S.; Schofer, C.; Weipoltshammer, K.; Pagani, M.; Lachner, M.; Kohlmaier, A.; Opravil, S.; Doyle, M.; Sibilia, M.; Jenuwein, T. *Cell* **2001**, *107*, 323−337.
(13) Lachner, M.; Jenuwein, T. *Curr. Opin. Cell Biol.* **2002**, *14*, 286−298.
(14) Saccani, S.; Natoli, G. *Genes Dev.* **2002**, *16*, 2219−2224.

JA038854H